Science of the Total Environment 945 (2024) 173910

Contents lists available at ScienceDirect

Science of the Total Environment

journal homepage: www.elsevier.com/locate/scitotenv

Review

Agri-food waste biosorbents for volatile organic compounds removal from air and industrial gases – A review

Patrycja Makoś-Chełstowska *, Edyta Słupek, Jacek Gębicki

Department of Process Engineering and Chemical Technology, Faculty of Chemistry, Gdansk University of Technology, 80–233 Gdańsk, Poland

HIGHLIGHTS

- Agri-food waste is valuable ecological adsorbents for air and industrial gas purification.
- Summary of methods to convert waste into biosorbents for the removal of volatile organic compounds (VOCs)
- Detailed explanation of the interactions between VOCs and biosorbents
- Developments in the application of biosorbents in air and industrial gas purification

GRAPHICAL ABSTRACT

ARTICLE INFO

Editor: Jay Gan

Keywords:
Adsorbents
Biochar
Agri-food waste
Gas purification
Volatile organic compounds

ABSTRACT

Approximately 1.3 billion metric tons of agricultural and food waste is produced annually, highlighting the need for appropriate processing and management strategies. This paper provides an exhaustive overview of the utilization of agri-food waste as a biosorbents for the elimination of volatile organic compounds (VOCs) from gaseous streams. The review paper underscores the critical role of waste management in the context of a circular economy, wherein waste is not viewed as a final product, but rather as a valuable resource for innovative processes. This perspective is consistent with the principles of resource efficiency and sustainability. Various types of waste have been described as effective biosorbents, and methods for biosorbents preparation have been discussed, including thermal treatment, surface activation, and doping with nitrogen, phosphorus, and sulfur atoms. This review further investigates the applications of these biosorbents in adsorbing VOCs from gaseous streams and elucidates the primary mechanisms governing the adsorption process. Additionally, this study sheds light on methods of biosorbents regeneration, which is a key aspect of practical applications. The paper concludes with a critical commentary and discussion of future perspectives in this field, emphasizing the need for more research and innovation in waste management to fully realize the potential of a circular economy. This review serves as a valuable resource for researchers and practitioners interested in the potential use of agri-food waste biosorbents for VOCs removal, marking a significant first step toward considering these aspects together.

* Corresponding author.
E-mail address: patrycja.makos@pg.edu.pl (P. Makoś-Chełstowska).

https://doi.org/10.1016/j.scitotenv.2024.173910
Received 28 April 2024; Received in revised form 6 June 2024; Accepted 8 June 2024
Available online 14 June 2024

1. Introduction

The volatile organic compounds (VOCs) significantly contribute to air pollution. Environmental Protection Agency (EPA) defines VOCs as organic substances with boiling points ranging from 50 to 260 °C and a high vapor pressure at room temperature. They can react with other substances in the atmosphere, contributing to phenomena such as photochemical fog and ozone depletion. VOCs also pose risks to the environment, human health, animals, and industrial facilities (U.S. Environmental Protection Agency (EPA), 2024). Industrial activities, such as process vessels, venting, piping and equipment leaks, wastewater streams, heat exchange systems, storage tank emissions, raw/finished product transportation, and domestic fuel combustion, contribute to the release of VOCs. Automobile exhaust poses the greatest threat to the environment (Hu et al., 2020; Mu et al., 2022; Hsu et al., 2022; Xue et al., 2022; Lu et al., 2022a; Liu et al., 2022a; Makoś et al., 2019).

Efficient capture of VOCs present in the air, fuels, and industrial gas streams is of utmost importance. VOCs can cause short-term discomfort and long-term health problems, including cancer and lung, liver, and kidney damage. Inhalation is the primary route of chemical exposure. In addition, VOCs contribute to indoor and outdoor air pollution (Davidson et al., 2021). Various methods can be used to treat gaseous streams, such as catalytic and thermal oxidation, adsorption, physical and chemical absorption, membrane separation, cryogenic separation, and biological separation (Huang et al., 2016a; Khan and Kr, 2000; Gan et al., 2022; Gong et al., 2018; Li et al., 2022a; Liang et al., 2020; Meena et al., n.d.; Zhang et al., 2022a). The advantages and limitations of various methods are summarized in Table S1. Physical adsorption is a highly regarded technique among established technologies, due to its high process efficiency and the absence of harmful chemicals (Ye et al., 2023). Additionally, this method offers the ability to repeatedly regenerate the adsorbent, due to the stability of the utilized materials (Makoś et al., 2020). Frequently utilized adsorbents in the purification of gaseous streams encompass activated carbon (Sigot et al., 2016; Zulkefli et al., 2019; Santos-Clotas et al., 2019; Bak et al., 2019; Surra et al., 2019; Gislon et al., 2013; Gil et al., 2015; Kwaśny and Balcerzak, 2016; Wang et al., 2019; Hernández et al., 2011; Gaj, 2020; Durán et al., 2018; Abdullahi et al., 2018), silica gel (Sigot et al., 2016, 2014; Bak et al., 2019; Wang et al., 2019; Grande et al., 2020; Meng et al., 2020) and zeolites (Sigot et al., 2016; Bak et al., 2019; Hernández et al., 2011; Abdullahi et al., 2018; Peluso et al., 2019; Cabrera-Codony et al., 2017; Alonso-Vicario et al., 2010; Irvan et al., 2018; Grande and Rodrigues, 2007; Kusrini et al., 2019). Nevertheless, traditional adsorbents prove inadequate in effectively treating specific VOCs with low molecular weight or polar characteristics (Hu et al., 2018; Kumar et al., 2019). These adsorbents exhibit shortcomings related to their poor thermal stability, flammability, and explosive properties. Consequently, advanced adsorbents including metal-organic frameworks and (Kumar et al., 2019) carbon-based nanomaterials (Kumar et al., 2020a) have emerged as promising materials for VOC capture. Despite their ability to address the aforementioned limitations, the preparation of advanced adsorbents is both expensive and intricate, rendering their use impractical in industrial settings.

Biosorbents are environmentally sustainable alternatives to conventional and advanced adsorption materials. Biosorption is a specific type of traditional adsorption technique in which the sorbent is derived from biological sources such as biomass, microorganisms, or animal waste. In contrast to classical adsorption techniques that rely on synthetic materials such as silica gel, activated carbon, or zeolites, the biosorption process involves a variety of mechanisms. These mechanisms may include physical interactions, such as electrostatic forces, van der Waals forces, and hydrogen bonds, as well as chemical binding, which can involve ionic and covalent bonds. Some proposed mechanisms for biosorption include absorption, surface adsorption, ion exchange, surface complexation, precipitation or microprecipitation, and mineral nucleation (Crini et al., 2019). The benefits of biosorption include cost efficiency. The estimated cost of biosorbents is approximately 0.5/kg, whereas the cost of conventional biosorbents can be as high as €100 to €250/kg, as reported in reference (Karić et al., 2022). In addition to cost-effectiveness, biosorbents offer several advantages. For instance, they can significantly reduce the amount of solid waste generated, possess sorption capacity comparable to commercial adsorbents, and potentially allow for the recycling of biomass when feasible (Crini et al., 2019; Karić et al., 2022). Despite these advantages, the inherent adsorption efficiencies of raw biosorbents are constrained by the changeable structure, which is influenced by the type of waste and their condition before undergoing processing (Dong et al., 2021; Ghanbari and Niu, 2019). Consequently, it is imperative to undertake targeted modifications aimed at augmenting the specific surface area of sorbents, thereby enhancing their adsorption capacities. Currently, biosorbents are increasingly employed in water and wastewater treatment (Karić et al., 2022). However, most published research has focused on the removal of heavy metals or inorganic substances from liquid streams (Zeghioud et al., 2022; Sheth et al., 2021; Qin et al., 2020; Elgarahy et al., 2021). There is limited literature describing the purification of gas streams using biosorbents. Scientific studies have primarily focused on the removal of inorganic pollutants such as H_2S, CO_2, NOx, and H_2O from air or gaseous industrial streams (Mohamad Nor et al., 2013; Jung et al., 2019; Premchand et al., 2023; Zhao et al., 2022). There has been significantly less research dedicated to the adsorption of VOCs including linear and aromatic volatile hydrocarbons, volatile organochlorine compounds, volatile methyl siloxanes, volatile oxygenates organic compounds, and volatile organosulfur compounds from gases.

A graph showing the number of papers published on biosorbents compared to papers dedicated to the removal of volatile organic compounds from gaseous streams versus water and wastewater using biosorbents is shown in Fig. 1.

Furthermore, there is a lack of structured knowledge in this area. This study addresses this gap by providing a literature review on the latest developments in the preparation and modification of biosorbents. The review encompasses their applications in removing VOCs. In addition, this paper discusses the main advantages and limitations of using biosorbents along with potential future prospects. The review papers were prepared based on articles found in the Scopus database. The publications considered in the literature review were published between 2014 and 2024.

2. Raw agri-food waste biosorbents characterization

Biosorbents exhibit diverse classifications, with one approach being based on their zoonotic or plant origin. Biosorbents derived from plants are commonly referred to as lignocellulosic biosorbents. Within this category, distinctions can be made between fruit, vegetable residues, and crop residues. Fig. 2 illustrates the primary types of agri-food waste biosorbents.

2.1. Animal waste-based biosorbents

Animal waste contains various substances capable of adsorbing VOCs, one of which is keratin from the scleroprotein group. Keratin is rich in cysteine, an amino acid that forms disulfide bridges between protein chains, thus providing strength and stability to its structure. This protein exhibits both α-helix and β-fold structures, providing protective and structurally stabilizing features (Wang et al., 2016; Khosa et al., 2013). The functional groups of keratin make it capable of forming hydrogen, ionic, and disulfide bonds, as well as hydrophobic interactions. The presence of disulfide bonds in keratin cross-links the polypeptide chain, rendering it insoluble in water, salts, diluted acids, and alkali solutions, contributing to its excellent mechanical resistance. The cysteine content in keratin varies, with soft keratin containing 2 % cysteine and hard-soft keratin containing up to 10–14 % or 22 %

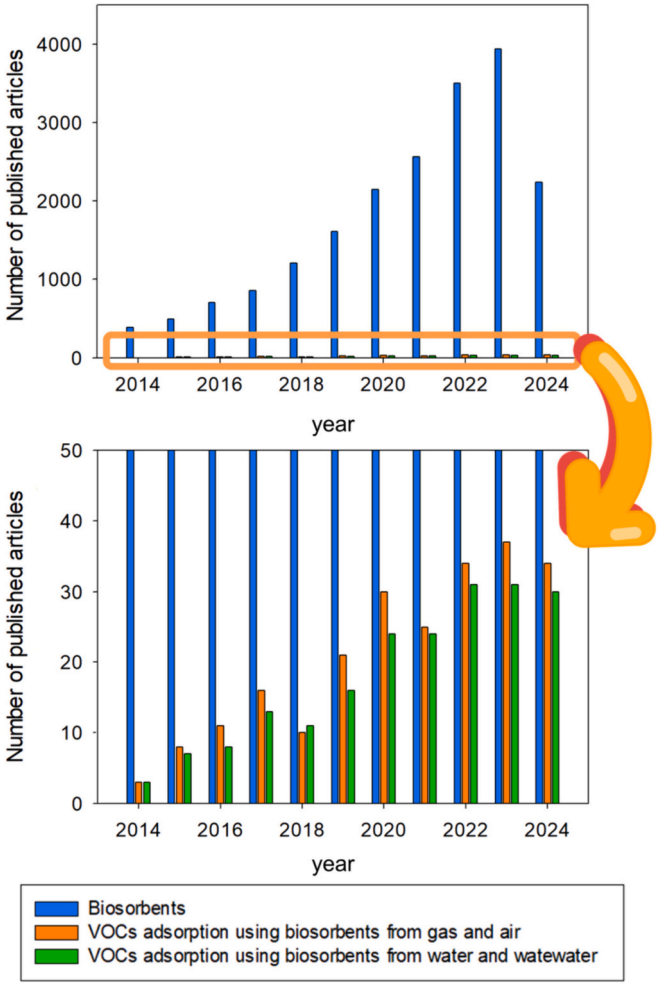

Fig. 1. Number of published papers between 2014 and 2024. The graphs were built using the Scopus database, from the topics biosorbents or biochar, adsorption, volatile organic compounds, water or wastewater, and air or gas (Access date: 05.06.2024).

cysteine (Donato and Mija, 2020; Aluigi et al., 2009; Chen et al., 2022). Biosorbents obtained from marine organisms, such as crab and shrimp shells, insect shells, fungi, algae, and protozoa, are rich in chitin, with varying chitin content depending on the source material. For instance, the crab shell of *Chinonecetes opilio* contains 26.7 % chitin along with other components such as proteins (29.2 %), ash (40.6 %), and lipids (1.4 %) on a dry weight basis (An et al., 2001; Liu et al., 2017a). Its high nitrogen content makes it a suitable amino-functional precursor for nitrogen-doped carbon synthesis via pyrolysis followed by activation. In this structure, repeated 2-(acetylamino)-2-deoxy-D-glucose units are present, and chitin possesses hydroxyl and acetyl groups that enable effective binding with VOCs. The appeal of chitin as a biosorbent lies not only in its abundance but also in its low cost, straightforward production process, flexible chemical distribution, and absence of waste products and secondary pollution, owing to its functional structure (Peter et al., 2021). Chitosan, a derivative of chitin renowned for its ability to capture VOCs, is a natural alkaline polysaccharide. Chitosan is obtained by partially deacetylating the acetamido groups within chitin. Despite the presence of functional groups, such as = O, —O—, -OH, and -NH_2, the VOCs adsorption efficiency of chitosan is low. Consequently, neither chitosan nor chitin are employed as standalone substances in VOC adsorption processes (Peter et al., 2021; Huo et al., 2024; Mohamed and Ouki, 2011). Fish scales have low concentrations of chitin, and their primary components are type I collagen and hydroxyapatite. Analysis showed that moisture and protein make up the majority of their weight,

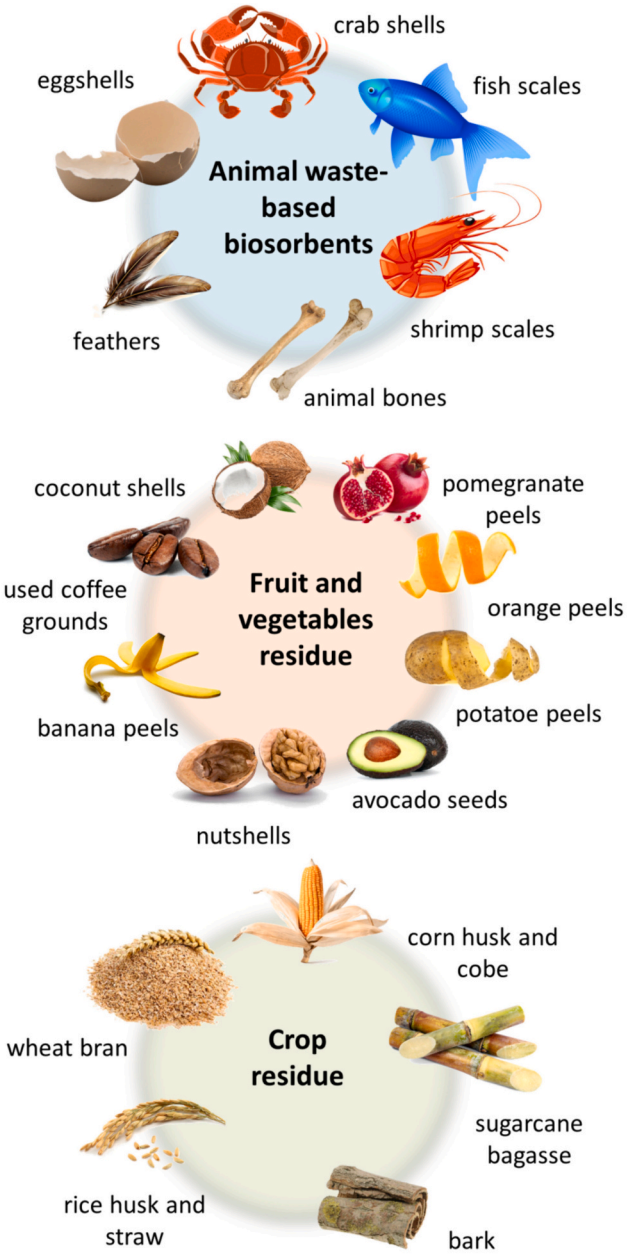

Fig. 2. Main groups of agri-food waste biosorbents used as adsorbents for VOCs removal from gas streams

with approximately 23 % attributed to proteins and low levels of lipid and carbohydrate content. The proportion of proteins increased with the weight and length of fish. Type I collagen is characterized by a triple-helical structure of G-X-Y, where Glycine is a constant amino acid and x and y vary. The amino acids in collagen contain functional groups that can interact with VOCs. Fish scales also contain hydroxyapatite, which can interact with VOCs through ionic and hydrogen bonding interactions (Fan et al., 2023; Salindeho et al., 2022). Eggshells consist of approximately 90–95 % $CaCO_3$ in the form of calcite, along with 1 % magnesium carbonate, 1 % calcium phosphate, and some organic compounds (Baláž, 2018). This composition renders them well suited as adsorbent materials for treating soils and water contaminated with metallic ions. The porous structure of eggshells further enhances their potential as adsorbents for removing various impurities from gas (Ahmad et al., 2021; Li et al., 2020a).

2.2. Lignocellulosic biosorbents

Biosorbents derived from lignocellulosic materials, which are typically sourced from plant substances and industry by-products, present a cost-effective solution for gas treatment. Lignocellulosic waste biosorbents consist primarily of cellulose, hemicellulose, and lignin (Fig. 3). The proportion of the main biosorbent components varies according to the type of plant material used. Table S2 summarizes the compositions of the lignocellulosic sorbents. Cellulose, a key component of lignocellulosic biosorbents, comprises β-D-glucopyranose sugar units and contributes to structural support (Berslin et al., 2022; Qiu et al., 2022). With a linear polymer structure resulting from the dehydration of glucose, cellulose forms microfibrils in the supramolecular structure through the intertwining of the crystalline and noncrystalline phases. In contrast, hemicellulose is a non-crystalline polysaccharide polymer with a lower degree of polymerization than cellulose. Lignin, characterized by its amorphous, heterogeneous, highly branched structure, is a multidimensional polymer composed of phenyl-propane monomers cross-linked with phenolic monomers (Tyagi and Anand, 2023). The content of the main components of lignocellulosic biosorbents gives them unique functional groups, that is, —O—, -OH, and =O, which are capable of forming non-covalent bonds. The structure of lignocellulosic biosorbents is porous, which is beneficial for the adsorption of organic pollutants from gas streams. However, pores are often too large to effectively capture small VOCs. In addition, lignocellulosic wastes are hydrophilic in nature, making them effective adsorbents for the removal of hydrophilic pollutants.

2.3. Biosorbents modification

Biosorbents can be utilized in their natural state without surface modifications (Ghanbari and Niu, 2019; Wu et al., 2022). This approach significantly reduced the cost and time required to prepare sorbents. However, the current applications of these biosorbents are primarily confined to the removal of moisture from gas. To improve the sorption properties and impart selectivity, it is important to modify the surface of biosorbents (Karić et al., 2022; Chong et al., 2023; Tariq et al., 2023). Fig. 4 provides a summary of the most popular surface modification methods. Fig. 5 shows the effects of each modification method on the structural properties of the biosorbents.

2.3.1. Thermal conversion

Lignocellulosic waste must undergo thermal treatment to produce activated carbon or biochar. These methods include pyrolysis, hydrothermal carbonization, torrefaction and gasification (Stöcker, 2023; Awasthi et al., 2023).

Pyrolysis is a primary method for thermally treating lignocellulosic materials (N et al., 2022). This process involves the breakdown of organic matter at elevated temperatures, usually ranging from 250 to 900 °C, and can be performed in the presence or absence of limited oxygen. During pyrolysis, cellulose, hemicellulose, and lignin are broken down into smaller molecules through depolymerization, fragmentation, and cross-linking, resulting in the production of various products in different phases, including solids, liquids, and gases. Pyrolysis is classified into three types: slow, fast and microwave pyrolysis, which are determined by the applied temperature and residence time (Dhyani and Bhaskar, 2018; Wang et al., 2017a). During slow pyrolysis, waste materials undergo a process in which temperatures range from 300 to 500 °C and the residence time can last from several minutes to days. This method is highly effective due to its ability to produce the maximum amount of solid products while minimizing the generation of gaseous and liquid products. Increasing the temperature usually results in a decrease in biochar yield and biogas production. In contrast, fast pyrolysis is designed specifically to convert lignocellulosic waste into bio-oil, which is highly valuable for energy production but not suitable for adsorbents. Conducted at temperatures ranging from 500 to 700 °C, this pyrolysis variant features rapid heating rates and shorter residence times, measured in seconds. These conditions result in a lower yield of the solid fraction, but the adsorbents exhibit a larger surface area and fewer functional groups on the surface. The process temperature can affect the properties of biosorbents, with higher temperatures enhancing the hydrophobicity of the adsorbents (Liang et al., 2016). Microwave pyrolysis is characterized by a temperature differential between the center and surface of the feedstock, leading to efficient heat transfer and a shorter reaction time compared to alternative thermochemical methods. While this technique yields smaller fractions of the liquid phase compared to other methods, its application is limited owing to its cost and the need for advanced equipment (Huang et al., 2016b; Zhang et al., 2017a; Tripathi et al., 2016). Consequently, microwave pyrolysis has not been widely adopted for the production of biosorbents from waste materials (Kan et al., 2016).

The process of hydrothermal carbonization involves subjecting lignocellulosic waste to water at high pressure and temperature (180–230 °C), in a sealed system. The pressure and temperature are carefully controlled to ensure the water remains in a liquid state during the process. This method, which is used to produce adsorbents, is gaining attention because it can utilize wet lignocellulosic waste without requiring an additional drying step. The process results in a high recovery of the solid fraction and operates at a relatively low temperature. Additionally, the obtained biosorbents produced contains a significant amount of oxygen-containing functional groups, making it suitable for adsorbing VOCs. Nevertheless, the primary constraints linked to this approach stem from the necessity of elevated pressure coupled with high temperatures and the expenses associated with the reactor. Consequently, the practical use of this method on an industrial scale is limited (Xiao et al., 2012; Funke and Ziegler, 2010).

Another process is torrefaction, sometimes referred to as mild pyrolysis. This method involves exposing lignocellulosic biomass to an inert atmosphere at temperatures ranging from 200 to 300 °C, resulting in the conversion of the biomass into a charcoal-like carbonaceous material (Yang et al., 2023; Jiang et al., 2021). During this process, depolymerization of the biomass occurs, which is influenced by the reaction time and temperature. Although biochar is not the primary product of torrefaction, the resulting material is suitable for the adsorption of pollutants due to its hydrophobic properties (Ivanovski et al., 2022; Sarker et al., 2021). This is because the disruption of hydroxyl groups prevents the formation of hydrogen bonds, resulting in the formation of non-polar unsaturated structures that provide long-term stability to the biosorbents without being susceptible to biological degradation (Ong et al., 2021).

2.3.2. Activation

2.3.2.1. Mechanical activation. The process of reducing the size of biosorption material to nanoscale particles has become an affordable and viable alternative activation method. Factors such as the ratio of ball-to-powder mass, rotation speed, and milling time all have a significant impact on the surface energy and particle size of the resulting nanobiosorbent. Nanobiosorbents have a much larger surface area, as well as unique pore shapes and sizes. The popularity of this mechanical activation method has grown due to its capability to produce novel nanomaterials without the use of solvents. While it is a commendable substitute for chemical activation processes, it has not yet gained widespread acceptance (Xiang et al., 2020; Lyu et al., 2020).

2.3.2.2. Physical activation. Physical activation is achieved by subjecting biosorbents to high-temperature gases, such as steam, CO_2, or a combination of air and oxygen, between 700 and 900 °C (Palniandy et al., 2019; Yang et al., 2021). In the gasification process, carbon is removed from the biosorbents, resulting in the formation of pores and an increase in surface area. This process is accomplished through the

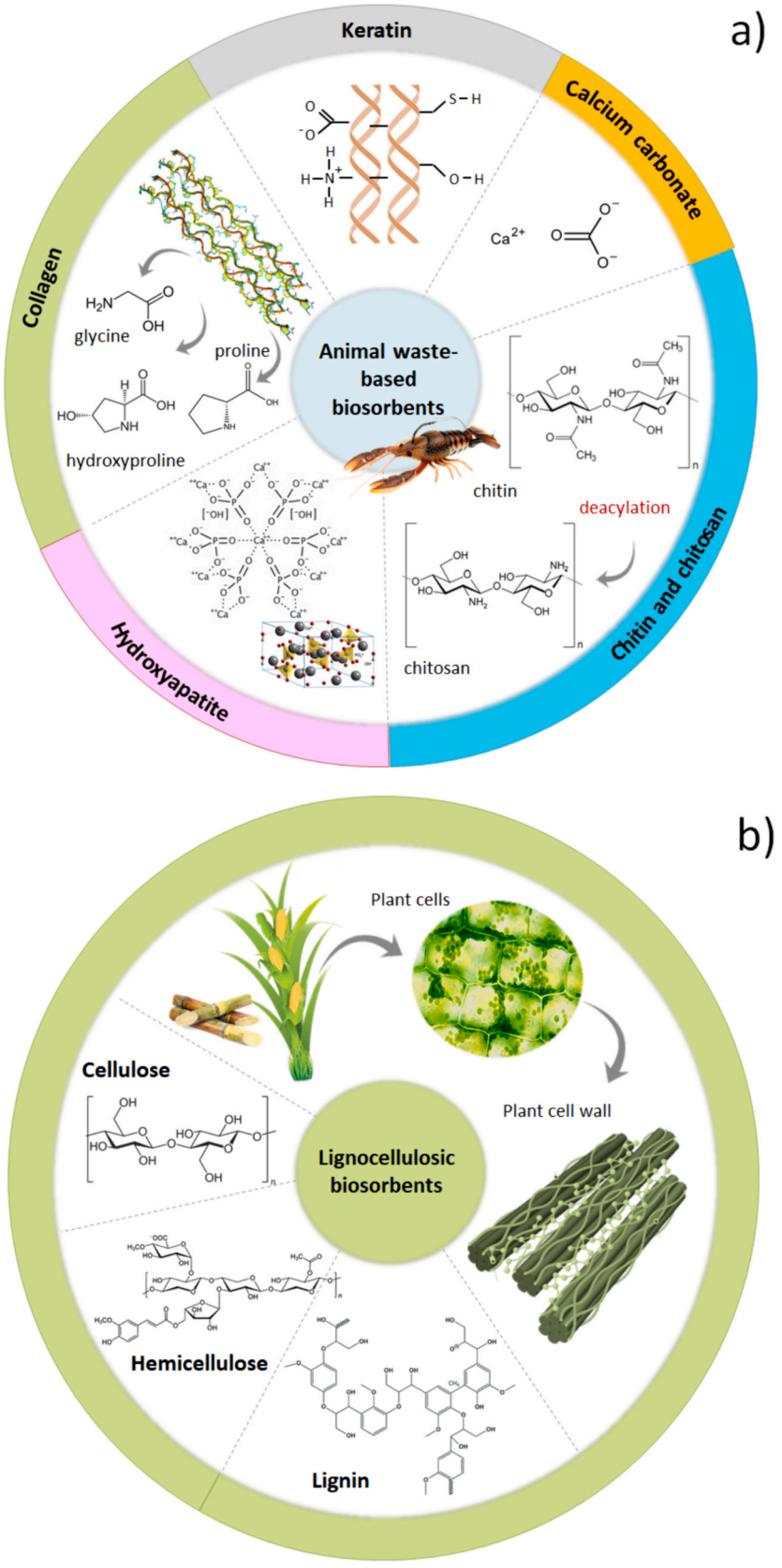

Fig. 3. The main substances present in various types of biosorbents.

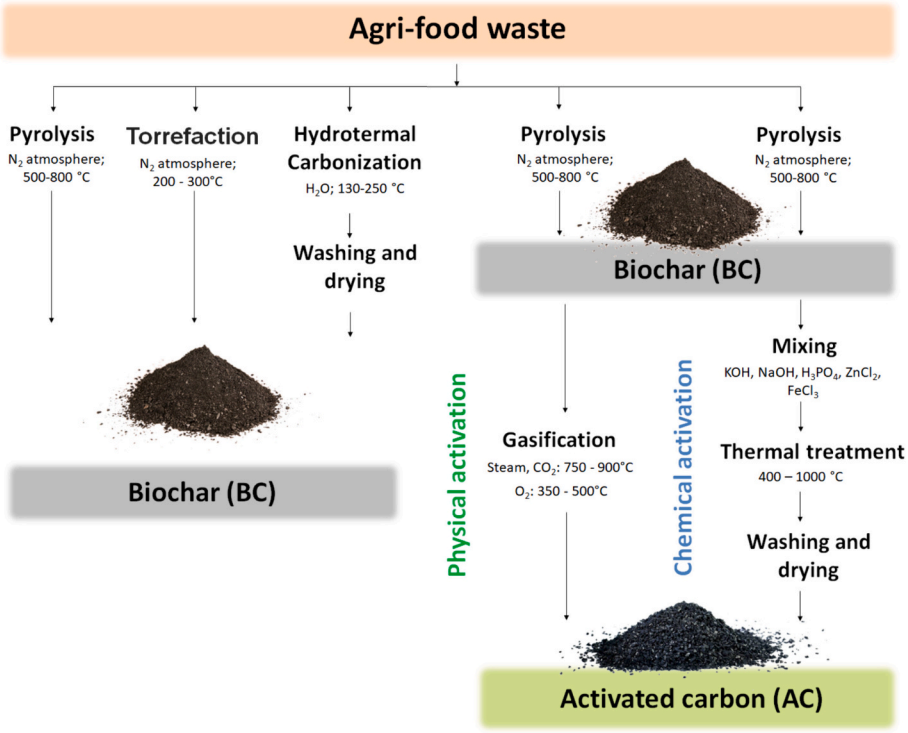

Fig. 4. Procedures for biosorbents preparation.

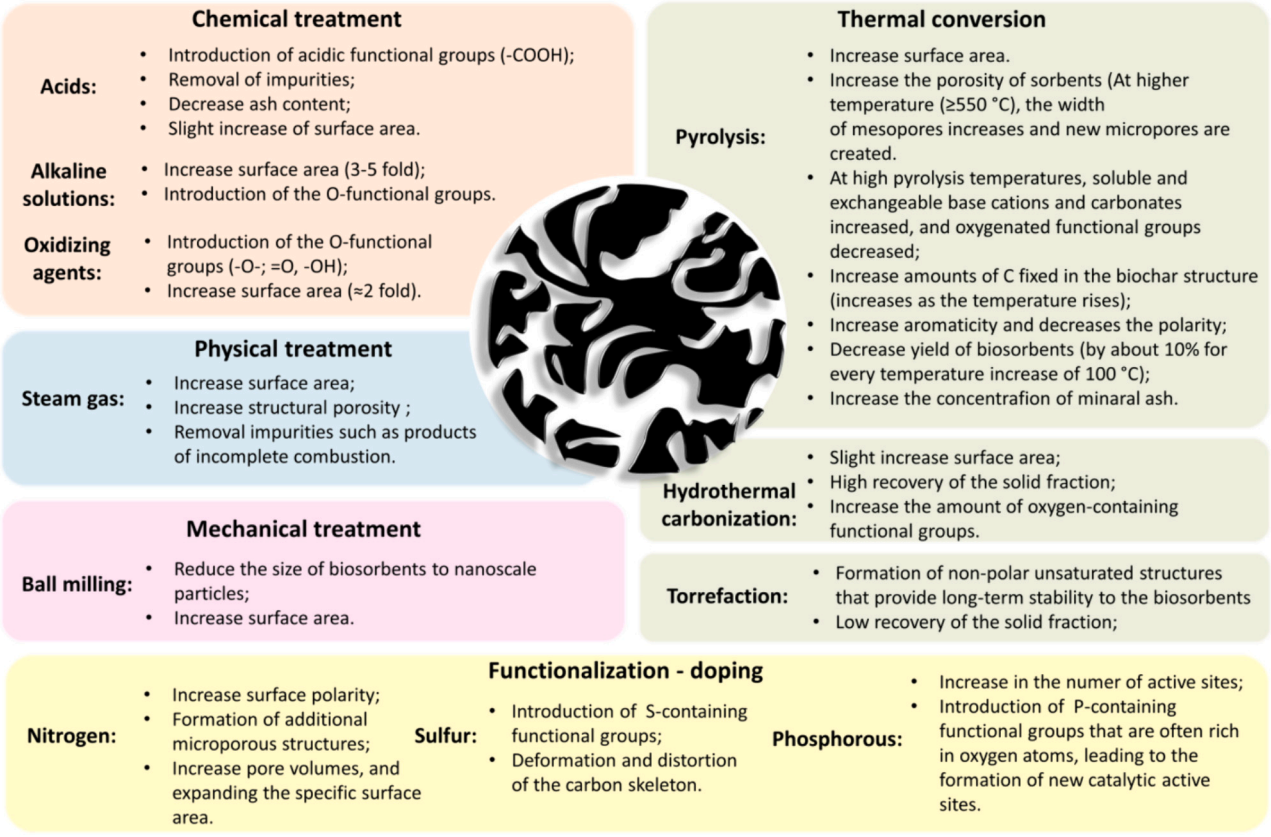

Fig. 5. The impact of different modification methods on the structural properties of biosorbents.

reaction of steam, CO_2, or Air/O_2 with carbon, which generates additional pores. The effectiveness of physical activation depends on various factors, including temperature, activation degree, precursor type, and activation agent. Higher activation temperatures and longer activation times generally lead to better porosity growth. However, this can also result in a wider distribution of pore sizes. Using air as the activation

agent can be challenging since the interaction between air and carbon-rich char tends to shift toward combustion if not properly controlled, leading to excessive ash formation and a reduced activated carbon yield. Physical activation has been shown to improve the specific surface area of biosorbents, but it does not result in changes to the functional groups of these materials. The presence of functional groups play a key role in the adsorption of VOCs (Sajjadi et al., 2019). For this purpose, chemical activation should be used.

2.3.2.3. Chemical activation. Chemical activation is a process in which a chemical substance, referred to as an activating agent, is used to activate biosorbents. This is followed by thermal conversion (Din et al., 2017; Sakhiya et al., 2020). The first category of activation reagents used were inorganic acids, such as H_2SO_4, HNO_3, H_3PO_4, and HCl. These acids alter the surface of biosorbents by introducing acidic functional groups and removing metallic impurities. Acids with high oxidation capabilities interact with the mineral components of biosorbents, creating voids between the carbon layers and increasing surface area. The type of acid, ratio of biosorbent to acid, and its concentration influence the development of active groups that bond with VOCs and the specific surface area. At higher concentrations, activators can form an extremely porous structure through intensified dehydration or condensation. However, excess activators can decrease adsorption capacity by occupying certain macroporous areas (Panwar and Pawar, 2022; Angin et al., 2013).

The optimal concentration of HCl for biosorbents is 0.2 M, as higher concentrations can impair the pore structure and decrease the adsorption capacity. Excessive activator amounts can compromise biosorbent properties owing to pore dissolution and breakage. Chemical activation offers advantages, such as lower temperature requirements, shorter treatment times, higher carbon yields, and increased surface area. It also exhibited well-developed and controlled microporosity. However, the use of strong acids, such as HCl, is environmentally harmful and costly because of their corrosive properties. The biosorbents must be thoroughly washed to remove excess activation agents. Acids, such as H_3PO_4 and H_2SO_4, can be used, with H_2SO_4 being more affordable. Boric acid is another effective weak acid for activating biosorbents by increasing the specific surface area through micropore formation during pyrolysis (Zhang et al., 2022b). The subsequent group of activating agents consists of oxidizing substances including ozone (O_3) hydrogen peroxide (H_2O_2) and potassium permanganate ($KMnO_4$). Additionally, oxidizing acids, such as nitric acid and phosphoric acid, may also be included in this category. Even at low temperatures, oxidants induces the formation of acidic binding sites, such as carboxylic, phenolic, lactonic, and carbonyl, on the surfaces of the biosorbents. This increase in oxygen-containing binding sites significantly enhanced the sorption capacity, reaching up to 22 times that of untreated biosorbents (Wang et al., 2023; Chen et al., 2024; Yakout, 2015; Jimenez-Cordero et al., 2015). Another class of chemical activators includes bases. Treating biochar with potassium hydroxide (KOH) followed by pyrolysis increases the surface area and enhances the porosity, resulting in an improved capacity for adsorbing contaminants from gas streams. Applying heat and activating with NaOH or KOH at temperatures ranging from 350 to 550 °C can open partially blocked pores and enlarge smaller pores (Panwar and Pawar, 2022; Gale et al., 2021). The final category of activators includes salts. Salt activation is characterized by a more environmentally benign and less corrosive nature than acid and base activation methods. Furthermore, stringent safety measures are imperative for acid and base activations, as highly acidic and basic activations pose the potential hazard of inducing furnace explosions due to the associated fumes. $ZnCl_2$, $FeCl_3$, NaCl are among the salts commonly employed as activating agents (Panwar and Pawar, 2022; Adeniyi et al., 2023).

2.3.3. Functionalization - doping

The doping of biosorbents involves the incorporation of heteroatoms such as nitrogen, phosphorus, sulfur, and metal oxides into the structure of the biosorbents. This procedure can markedly improve the characteristics of biosorbents, including their capacity to interact with various VOCs. The amount of doping is largely influenced by the doping procedure and the types of heteroatoms, and it typically ranges from 0.12 to 9.1 % (*w*/w) (Chen et al., 2017; Sun et al., 2023). Methods for producing heteroatom-doped biosorbents can be divided into two categories: pre-decoration doping and post-decoration doping. Pre-decoration doping typically involves processes such as pyrolysis or hydrothermal carbonization. On the other hand, post-decoration doping involves modifying existing biosorbents, including post-carbonization and impregnation. The most prevalent method of post-carbonization involves adding a source of heteroatoms and an additive, allowing for simultaneous doping and activation of biosorbents (Sun et al., 2023).

Among the various available methods, nitrogen doping has gained popularity and has been extensively studied owing to its lack of electronic effects (Feng et al., 2023; Kasera et al., 2022; Lu et al., 2022b). Nitrogen, with its localized unpaired electrons, can enhance the electron density of adjacent carbon atoms, making nitrogen doping a straightforward process. Furthermore, nitrogen doping can enhance the π-electron flow of sp^2 carbons, increase the number of functional groups, and create defects (Chen et al., 2016). As a result, the surface polarity of carbon materials increases, making them more appealing to polar adsorbents. The primary agents used for nitrogen doping include ammonia, urea, ammonium bicarbonate, and other nitrogen-containing organic compounds. NH_3 is typically used as an external source of nitrogen to facilitate its introduction into biosorbents, and its content can reach approximately 10 wt% (Chen et al., 2016; Deng et al., 2015). The main nitrogen-containing functional groups in biosorbents are pyridinic N, pyrrolic N, quaternary N, and pyridone N-oxide. These are formed as follows: ammonia initially reacts with -OH and -C=O in biosorbents to produce pyridinic-N and pyrrolic-N, after which pyridinic-N is transformed into quaternary-N through a polymerization reaction (Deng et al., 2015). The modification of nitrogen-based chemicals with functional groups can significantly enhance the adsorption capacity of biosorbents. Nitrogen-doped modification has the advantage of creating additional microporous structures, increasing pore volumes, and expanding the specific surface area of adsorbents (Feng et al., 2023; Pi et al., 2021; Liu et al., 2024; Niu et al., 2019).

Sulfur is another heteroatom that is commonly used in the modification of biosorbents (Sun et al., 2023). The primary chemical agents employed for sulfur doping are H_2SO_4, H_2S, SO_2, and sulfur-containing polymers (Kiciński et al., 2014). In contrast to nitrogen, sulfur and carbon atoms have similar charges, leading to minimal polarization of the chemical bonds between sulfur and carbon atoms (Liu et al., 2017b). This suggests that the local structure did not affect the electron density of the carbon atoms (Shi et al., 2017). The larger size of sulfur atoms and longer chemical bonds between carbon and sulfur atoms cause the carbon skeleton to be distorted and deformed. Additionally, the spacing between the graphite layers increased and there were a considerable number of defects and strains in the carbon skeleton. These defects and strains change the original charge distribution, leading to the formation of more active sites in the carbon material, which is useful for the adsorption of VOCs (Wang et al., 2020a; Su et al., 2018; Wohlgemuth et al., 2012). Despite the observed increase in the number of active sites, the precise mechanism of the material transfer remains ambiguous.

By adding phosphorus to biosorbents, their activity can be improved more effectively, as phosphorus has a lower electronegativity and larger covalent radius than nitrogen and sulfur (Sun et al., 2023). This resulted in an increase in the number of active sites. Additionally, phosphorus doping introduces P-containing functional groups that are often rich in oxygen atoms, leading to the formation of new catalytic active sites during the doping process (Zhou et al., 2020; Khan et al., 2020; Wang et al., 2017b).

3. Application of biosorbents for VOCs removal from air and industrial gases

3.1. Linear and aromatic volatile hydrocarbons

Linear and aromatic volatile hydrocarbons are VOCs that significantly affect air quality. Their presence in the environment is due to various human activities and industrial processes (Zhou et al., 2023; Wang, 2020; Geldenhuys et al., 2022; Almohammadi et al., 2021; Fiebig et al., 2014). It is worth noting that aromatic hydrocarbons such as benzene, toluene, ethylbenzene, and xylenes (BTEX) negatively affect the cardiovascular, reproductive, or nervous systems (Mallah et al., 2022). In addition, these compounds are classified as carcinogenic, mutagenic, and toxic (Kuranchie et al., 2019) (Table 1).

Kim et al. analyzed the impact of the type of impregnating agent on the adsorption capacities of BTX. The study used activated coconut shells treated with various acids and bases. The adsorption capacity of activated carbon was found to be influenced by the impregnation process, which altered its structural properties. The highest adsorption capacity was observed for the activated carbon impregnated with 1 % H_3PO_4. This may be due to the narrowing of the micropores in the activated carbon structure caused by phosphoric acid, which creates a favorable environment for the adsorption of small-molecule pollutants such as B. This study found that the adsorption capacity decreased with increasing pollutant particle size. Therefore, the highest adsorption capacity was observed for benzene at 500.68 mg/g, whereas the lowest was for T at 373.2 mg/g (Kim et al., 2006). In subsequent studies, the Martinez de Yuso used almond shells to capture toluene. These studies indicated that activated carbons prepared at lower activation temperatures (400–467 °C) showed the highest adsorption capacity of 637.98 mg/g. Authors observed that humidity in the gas decreased the amount of T adsorbed by 9–46 % (Martínez De Yuso et al., 2013). Cheng et al. conducted research on the use of pistachio shells as biosorbents for T removal. This study found that nitrogen-doped biochar had a higher adsorption capacity for toluene, with 80 % retention, even under humid conditions. The increased specific surface area and nitrogen content of the biochar surface contribute to the selective adsorption of toluene over water vapor (Cheng et al., 2023). Yang et al. activated shaddock peel with KOH at molar ratios ranging from 1:1 to 1:4. These studies confirmed that increasing the molar ratio of the activator to the amount of raw biosorbent favorably affects the formation of a more porous structure of activated carbon. The obtained microporous structure increased the adsorption capacities of B from 195.71 to 1555.1 mg/g and T from 189.2 to 1795.0 mg/g, respectively (Yang et al., 2022). Similar studies were carried out by He et al., who obtained activated carbon from a lignin-based pitch. The biomass was activated using KOH at a molar ratio of 1:5. The tests obtained a maximum value of B adsorption at 1244.9 mg/g. Both research presents an environmentally friendly, cheap, and innovative approach to producing high-performance activated carbons through activation with KOH (He et al., 2021). Other studies used bamboo-based activated carbon as an alternative medium for dynamic VOC adsorption. In subsequent studies using bamboo-based biomass, activation was performed using microwave pyrolysis and an activator in the form of $FeCl_3$ (Lin et al., 2024). Studies have shown that the addition of $FeCl_3$ plays a dual role in pyrolysis for biochar production, acting as a microwave absorber to facilitate fast pyrolysis, and as a catalyst to improve the formation of a microporous structure, thereby increasing the hydrophobicity of biochar. Lin's research confirms that biochar produced by the microwave pyrolysis has a B and T adsorption capacity of 136.6 and 94.6 mg/g.

In the next studies using bamboo-based biomass, various activating agents have been used to prepare activated carbons, such as 80 % (*w/v*) H_3PO_4 and 30 % $ZnCl_2$ solutions, or activating using steam or CO_2 (Hu et al., 2017). Selecting the activating agent was key in determining the adsorption capacity, surface properties, and microporosity of monolithic activated carbon samples made of bamboo. Using acid combined with treatment at elevated temperatures reduced the number of surface oxygen-containing groups, improving hydrophobicity and reducing microporosity. The obtained size of the micropores in the sample after activation with H_3PO_4 acid most likely closely corresponded to the size of the adsorbate molecules. Acid activating-activated carbon exhibited a relatively short permeation time however they had the character's highest calculated dynamic adsorption capacity of 350 mg/g. In subsequent research, Rong's team focused on converting bamboo chars into porous graphitized carbons with desirable textural properties and hydrophobicity for the efficient adsorption of VOC (Rong et al., 2023). This study was conducted using a KOH-promoted $NiCl_2$ catalyst. The process involved the decomposition and reduction of $NiCl_2$ at 500 °C to obtain a product with a high graphitization level and well-developed micro mesoporosity. The obtained biosorbent had a specific surface area of 2181 m^2/g and a low surface O/C atomic ratio of 0.038. The research showed that the obtained structure of the activated carbons has improved π-π interactions and dispersion forces, which contribute to the selectivity of the adsorption of toluene and cyclohexane. Moreover, the tests showed that in dry conditions the adsorption capacity of toluene and cyclohexane was 617.07 and 319.77 mg/g, respectively. This research also described the regeneration process of biosorbents.

3.2. Volatile organochlorine compounds

Volatile organochlorine compounds (VOXs) are a particularly challenging group of chemicals often found in biogas and waste gases from industries, such as paint production, plastic manufacturing, foam production, and electronics (Almomani et al., 2018, 2021; Bailón et al., 2009; Makoś-Chełstowska et al., 2021; Salazar Gómez et al., 2016). Prolonged exposure to these substances can lead to uncertain health consequences. If atmospheric VOXs emissions are not controlled, they can contribute to the creation of photochemical smog and global warming. Furthermore, these compounds pose technological challenges because of their highly corrosive nature (Buekens and Huang, 1998).

Cosnier et al. investigated activated carbon prepared from coconut shells using steam activation at 850 °C to remove dichloromethane (DCM) and trichloroethylene (TCE) from a nitrogen stream. The coconut shell activated carbon was found to have a highly developed surface area of 2278 m2/g, which is thought to have contributed to the high adsorption capacity of VOXs (DCM = 2.69 mmol/g and TCE = 6.89 mmol/g). In addition, authors observed a significant effect of moisture on the sorption capacity of biosorbents as well as the high competitiveness of VOX and water removal. When water is pre-adsorbed, DCM and TCE molecules displace them from the active sites on the surface of the sorbents. However, during the simultaneous adsorption of water and VOX, biosorbent-water and biosorbent-VOX interactions were observed, causing a decrease in the sorption capacity of the biosorbents (Cosnier et al., 2006). The same biosorbent was tested for its chlorobenzene (CB) and T sorption capacities. To activate the biosorbent, HCl was used following the heat treatment and steam activation. The authors found that adsorption was primarily due to non-specific dispersive forces, known as London forces, and short-range repulsive energies, referred to as the Lennard-Jones (L-J) potential. The adsorption performance and capacity were influenced by the nature and polarizability (α) of the adsorbate. Chlorobenzene's greater relative mass endows it with higher adsorption potential (Zhao et al., 2018). In another study, corn stalks were examined for their ability to remove VOX after being treated with a pyrolysis at various temperatures, and the results were compared to those of commercial rice-husk-based biochar. The study found that the hydrophobic and electrostatic interactions of the adsorbents, including π–π interactions and electron donor-acceptor interactions, were the primary factors responsible for the adsorption process. Although the specific surface area of the rice husk biosorbents was higher, the corn stalks subjected to pyrolysis at 500 °C showed a higher adsorption capacity for all VOXs. Other studies have found similar results related to the adsorption of VOCs by pecan-and almond shell-based granular

Table 1
Summary of the application of biosorbents for VOCs removal from air and industrial gases.

Raw biosorbent	Surface modification	Biosorbent characterization	Gas matrix	Adsorbate	Adsorption conditions	Isotherm	q_{max}	Regeneration and multiple use of BS	Ref.
Linear and aromatic volatile hydrocarbons									
Coconut shell	Activation using KOH	S_{BET} = 478.0 m^2/g V_t = 0.61 cm^3/g	n.d.	B,T	T = 30 °C C_0 = 50–250 mg/L m_{BS} = 0.1 g	Langmuir, Freundlich Temkin	q_B = 212.77 mg/g q_T = 238.10 mg/g q_B = 344.83 mg/g q_T = 357.14 mg/g	Microwave regeneration at 600 W, nitrogen flow at 300 mL/min and time 3 min. 5 cycles	(Mohammed et al., 2015)
Coconut shell	Activation using KOH and NH_3	S_{BET} = 361.8 m^2/g V_t = 0.16 cm^3/g							
Coconut shell	Pyrolysis (N_2, 1173 K) HCl activation	S_{BET} = 1137 m^2/g V_{mic} = 0.430 cm^3/g V_t = 0.480 cm^3/g 40–60 mesh	Air	T	Flow rate: 2 L/min T = 30 °C C_0 = 80 ppm m_{BS} = 1.2 cm^3	Langmuir Tòth Dubinin–Astakhov	q_T = 272 mg/g	n.d.	(Zhao et al., 2018)
Coconut shell	10 M HNO_3 activation 70 °C for 2 h	S_{BET} = 528 m^2/g V_t = 0.170 cm^3/g 60–80 mesh C/O/N 95.26/4.17/0.57 %	Air	o-X	Flow rate: 45 mL/min T = 27 °C C_0 = 2176–2239 mg/m^3 m_{BS} = 2 g	BET	$q_{o\text{-}X}$ = 187 mg/g	n.d.	(Li et al., 2011)
Coconut shell	6.6 M $NH_3{\cdot}H_2O$ activation 70 °C for 2 h	S_{BET} = 868 m^2/g V_t = 0.176 cm^3/g 60–80 mesh C/O/Mg/Al/N 96.63/1.12/0.09/0.13/0.31 %					$q_{o\text{-}X}$ = 281 mg/g		
Coconut shell	1 wt% H_3PO_4 activation 25 °C for 1 h	S_{BET} = 1109 m^2/g V_{mic} = 0.43 cm^3/g V_{mes} = 0.09 cm^3/g V_t = 0.52 cm^3/g 30–35 mesh	He	T	Flow rate: 40 mL/min T = 25 °C C_0 = 10,000–15,000 ppm m_{BS} = 0.2 g	Type I adsorption isotherms	q_T = 4.21 mmol/g	Programmed desorption: 25 to 300 °C at a rate of 10 °C/min in He atmosphere	(Kim and Ahn, 2010)
Coconut shell	5 wt% HNO_3 activation 25 °C for 1 h	S_{BET} = 867 m^2/g 30–35 mesh	He	B,T,o-X,m-X, p-X	Flow rate: 40 mL/min T = 25 °C C_0 = 10,000–15,000 ppm m_{BS} = 0.2 g	Langmuir Freundlich	q_B = 4.72 mmol/g q_T = 3.08 mmol/g $q_{o\text{-}X}$ = 5.16 mmol/g $q_{m\text{-}X}$ = 3.91 mmol/g $q_{p\text{-}X}$ = 3.93 mmol/g q_B = 5.13 mmol/g q_T = 3.17 mmol/g $q_{o\text{-}X}$ = 4.40 mmol/g $q_{m\text{-}X}$ = 3.86 mmol/g $q_{p\text{-}X}$ = 4.35 mmol/g	Programmed Desorption: 25 to 300 °C at a rate of 10 °C/min in He atmosphere	(Kim et al., 2006)
	5 wt% H_2SO_4 activation 25 °C for 1 h	S_{BET} = 840 m^2/g 30–35 mesh							

(*continued on next page*)

Table 1 (*continued*)

Raw biosorbent	Surface modification	Biosorbent characterization	Gas matrix	Adsorbate	Adsorption conditions	Isotherm	q_{max}	Regeneration and multiple use of BS	Ref.
							$q_B = 4.00$ mmol/g $q_T = 2.25$ mmol/g		
	5 wt% HCl activation 25 °C for 1 h	$S_{BET} = 718$ m^2/g 30–35 mesh					$q_{o\text{-}X} = 3.85$ mmol/g $q_{m\text{-}X} = 3.06$ mmol/g $q_{p\text{-}X} = 3.49$ mmol/g		
							$q_B = 6.41$ mmol/g $q_T = 4.05$ mmol/g		
	5 wt% H_3PO_4 activation 25 °C for 1 h	$S_{BET} = 719$ m^2/g 30–35 mesh					$q_{o\text{-}X} = 4.92$ mmol/g $q_{m\text{-}X} = 4.11$ mmol/g $q_{p\text{-}X} = 5.19$ mmol/g		
							$q_B = 5.69$ mmol/g $q_T = 3.63$ mmol/g		
	5 wt% CH_3COOH activation 25 °C for 1 h	$S_{BET} = 984$ m^2/g 30–35 mesh					$q_{o\text{-}X} = 4.52$ mmol/g $q_{m\text{-}X} = 6.21$ mmol/g $q_{p\text{-}X} = 4.18$ mmol/g		
							$q_B = 4.52$ mmol/g $q_T = 2.87$ mmol/g		
	5 wt% KOH activation 25 °C for 1 h	$S_{BET} = 668$ m^2/g 30–35 mesh					$q_{o\text{-}X} = 4.11$ mmol/g $q_{m\text{-}X} = 3.64$ mmol/g $q_{p\text{-}X} = 4.31$ mmol/g		
							$q_B = 3.81$ mmol/g $q_T = 2.73$ mmol/g		
	5 wt% NaOH activation 25 °C for 1 h	$S_{BET} = 636$ m^2/g 30–35 mesh					$q_{o\text{-}X} = 4.04$ mmol/g $q_{m\text{-}X} = 4.50$ mmol/g $q_{p\text{-}X} = 3.92$ mmol/g		
Bamboo	5 % $FeCl_3$ Activation Pyrolysis (N_2, 650 °C)	$S_{BET} = 455.9$ m^2/g C/H/N/O 67.16/1.75/0.65/30.44 %	N_2	B,T	T = 25 °C $P/P_0 < 0.1$ $m_{BS} = 100$–150 mg	Type II and IV isotherms	$q_B = 136.6$ mg/g $q_T = 94.6$ mg/g	n.d.	(Lin et al., 2024)

(*continued on next page*)

Table 1 (*continued*)

Raw biosorbent	Surface modification	Biosorbent characterization	Gas matrix	Adsorbate	Adsorption conditions	Isotherm	q_{max}	Regeneration and multiple use of BS	Ref.
Bamboo	$NiCl_2$-$6H_2O$ activation KOH activation Pyrolysis (N_2, 500 °C)	S_{BET} = 2181 m^2/g V_{mic} = 0.66 cm^3/g V_{mes} = 0.62 cm^3/g V_t = 1.28 cm^3/g	N_2	T,CH	Flow rate: 150 mL/min *T* = 25 °C C_0 = 1000 ppm m_{BS} = 50 mg	Langmuir	q_T = 6.74 mmol/g q_{CH} = 4.43 mmol/g	Thermal regeneration at 90 °C for 2 h under a N_2 flow if 50 mL/min	(Rong et al., 2023)
Bamboo	KOH activation Pyrolysis (N_2, 700 °C)	S_{BET} = 2165 m^2/g V_{mic} = 0.87 cm^3/g V_{mes} = 0.130 cm^3/g V_t = 1.09 cm^3/g 0.5–1.0 mesh					q_T = 6.31 mmol/g q_{CH} = 4.74 mmol/g		
Bamboo	80 % (w/v) H_3PO_4 activation Pyrolysis (N_2, 400 °C,1 h)	S_{BET} = 1418 m^2/g S_{mic} = 606 cm^2/g C/O/Si/P 88.35/8.85/0.59/2.2 %	N_2	T	Flow rate: 150 mL/min *T* = 25 °C C_0=,000 ppm m_{BS} = 300 mg	n.d.	q_T = 350 mg/g	n.d.	(Hu et al., 2017)
Bamboo	Pyrolysis (N_2, 450 °C)	S_{BET} = 10.2 m^2/g	N_2	T,CH	Flow rate: 50 mL/min *T* = 20 °C	Pseudo-first and second order model	q_T = 62.25 mg/g q_{CH} = 53.72 mg/g	Thermal regeneration at 150 °C for 2 h under a N_2 flow if 50 mL/min 5 cycle	(Zhang et al., 2017b)
Sugarcane bagasse	Pyrolysis (N_2, 300 °C)	S_{BET} = 5.2 m^2/g					q_T = 65.54 mg/g q_{CH} = 68.42 mg/g		
Brazilian pepper wood	Pyrolysis (N_2, 450 °C)	S_{BET} = 0.7 m^2/g					q_T = 52.03 mg/g q_{CH} = 64.26 mg/g		
Sugar pepper wood	Pyrolysis (N_2, 600 °C)	S_{BET} = 2.6 m^2/g					q_T = 48.26 mg/g q_{CH} = 22.12 mg/g		
Hickory wood	Pyrolysis (N_2, 600 °C)	S_{BET} = 289 m^2/g					q_T = 56.84 mg/g q_{CH} = 49.74 mg/g		
Corn stalk (CS)	CS:agate balls 3:200 mass ratio – 300 rpm, 5 h H_2O_2 activation	S_{BET} = 345.41 m^2/g V_{mic} = 0.1586 cm^3/g V_t = 0.0287 cm^3/g C/H/O/N 66.49/2.62/23.98/1.09 % 40–100 mesh	N_2	B, m-X, o-X, p-X	Flow rate: 50 mL/min *T* = 25 °C V_B = 0.1247 mL $V_{m\text{-}X}$ = 0.1276 mL $V_{o\text{-}X}$ = 0.1142 mL $W_{p\text{-}X}$ = 0.1305 mL m_{BS} = 0.01 g	Pseudo-first and second-order models	q_B = 108.86 mg/g $q_{m\text{-}X}$ = 109.74 mg/g $q_{o\text{-}X}$ = 100.07 mg/g $q_{p\text{-}X}$ = 111.79 mg/g	Thermal regeneration at 200 °C 5 cycles	(Zhang et al., 2021)
Shaddock peel	KOH/C mass ratio 4 activation 800 °C Pyrolysis (N_2, 589 °C)	S_{BET} = 3358 m^2/g	N_2	B,T	Flow rate: 50 mL/min *T* = 25 °C P/P_o = 0.1	Langmuir	q_B = 1295.3 mg/g q_T = 1427.9 mg/g	Thermal regeneration at 150 °C in a vacuum Time 2 h 5 cycles	(Yang et al., 2022)
Cotton stalk	KOH/C mass ratio 4 activation 900 °C Pyrolysis (N_2, 603 °C)	S_{BET} = 2636 m^2/g V_{micro} = 1.67 cm^3/g	N_2	B,T			q_B = 1555.1 mg/g q_T = 1795.0 mg/g		
Elaeagnus angustifolia seeds	150 % ratio impregnation 48 h Pyrolysis (N_2, 500 °C,1 h)	S_{BET} = 1836 m^2/g V_{micro} = 0.12 cm^3/g V_t = 1.03 cm^3/g	N_2	B	Flow rate: 0.05–0.12 L/min *T* = 25–50 °C C_0 = 9.95–14.85 ppm m_{BS} = 0.1–0.75 g mesh = 180–500 μm	Pseudo-First Order and Pseudo-Second Order kinetic models. Langmuir, Freundlich and Dubinin-Radushkevich model	q_B = 49.98 mg/g	n.d.	(Kutluay et al., 2019)

(*continued on next page*)

Table 1 (*continued*)

Raw biosorbent	Surface modification	Biosorbent characterization	Gas matrix	Adsorbate	Adsorption conditions	Isotherm	q_{max}	Regeneration and multiple use of BS	Ref.
Corncob	$ZnCl_2$ activation 1:1 impregnation ratio, 550 °C	S_{BET} = 1501.0 m^2/g V_{mic} = 0.612 cm^3/g V_{mes} = 0.130 cm^3/g V_t = 0.742 cm^3/g	Air N_2	T T, p-X	Flow rate: 500 mL/min T = 25 °C C_0 = 3000 mg/m^3 m_{BS} = 0.3 g Flow rate: 0.2 L/min m_{BS} = 0.5 ± 0.01 g	Langmuir Freundlich Sips Toth Redlich–Peterson Pseudo-first order Pseudo-second order Elovich Model Intraparticle diffusion model	q_T = 414.6 mg/g	Thermal regeneration at 65 °C with nitrogen flow at 0.2 L/min and pressure at 11 kPa. 5 cycles Thermal regeneration at 95 °C with N_2 stream 5 cycle	(Zhu et al., 2018) (Mosleh and Rajabi, 2024)
Wheat straw (WS)	1 M, 1 % *w/v* HCL - 50 rpm, 4 h, 25 °C 1 % w/v - NaOH - 200 rpm, 24 h, 25 °C 3 g/L, 1 % w/v- $C_7H_6O_2$ - 200 rpm, 24 h, 25 °C impregnation	S_{BET} = 98.17 m^2/g V_t = 0.1736 cm^3/g C/H/O 60.85/4.87/34.28 %					q_{eqT} = 125.25 mg/g $q_{eqp\text{-}X}$ = 149.08 mg/g		
Almond shell	89 % H_3PO_4/AS 1.17 mass ratio activation Pyrolysis (N_2, 467 °C, 45 min)	S_{BET} = 1117 m^2/g V_{mic} = 0.181 cm^3/g V_{mes} = 0.494 cm^3/g V_t = 0.724 cm^3/g 0.2–1 mm	n.d.	T	T = 25 °C C_0 = 500 ppm m_{BS} = 100 mg	Langmuir	q_T = 6.924 mmol/g	Thermal regeneration at 150 °C in N_2 atmosphere	(Martínez De Yuso et al., 2013)
Pistachio shells (PS)	PS: $NaHCO_3$ 2:1 mass ratio activation Pyrolysis (N_2,700 °C,2h)	S_{BET} = 23 m^2/g V_{mic} = 0.01 cm^3/g V_t = 0.03 cm^3/g N/C/H/O 0.54/74.24/1.06/24.16 %	N_2	T	Flow rate: 1 L/min *T* = 40 °C C_0 = 110 ± 5 mg/m^3 m_{BS} = 0.2 g RH = 0 %	Type I adsorption isotherms	q_T = 3.58 mg/g	n.d.	(Cheng et al., 2023)
	PS: K_2CO_3 2:1 mass ratio activation Pyrolysis (N_2,700 °C,2h)	S_{BET} = 758 m^2/g V_{mic} = 0.29 cm^3/g V_t = 0.31 cm^3/g N/C/H/O 0.3/66.95/2.19/30.56 %					q_T = 123.01 mg/g		
	PS:$NaHCO_3$: K_2CO_3 2:1:1 mass ratio activation Pyrolysis (N_2,700 °C,2h)	S_{BET} = 704 m^2/g V_{mic} = 0.28 cm^3/g V_t = 0.31 cm^3/g N/C/H/O 3.2/60.6/1.21/34.99 %					q_T = 107.03 mg/g		
	PS: melamine: $NaHCO_3$ 5:1:2.5 mass ratio activation Pyrolysis (N_2,700 °C,2h)	S_{BET} = 582 m^2/g V_{mic} = 0.23 cm^3/g V_t = 0.25 cm^3/g N/C/H/O 3.97/76.08/1.18/18.77 %					q_T = 77.15 mg/g		
	PS: melamine: K_2CO_3 5:1:2.5 mass ratio activation Pyrolysis (N_2,700 °C,2h)	S_{BET} = 1832 m^2/g V_{mic} = 0.72 cm^3/g V_t = 0.80 cm^3/g N/C/H/O 2.76/74.93/2.9/19.41 %					q_T = 223.56 mg/g		
	PS: melamine: $NaHCO_3$:K_2CO_3 5:1:2.5:2.5 mass ratio activation Pyrolysis (N_2,700 °C,2h)	S_{BET} = 847 m^2/g V_{mic} = 0.34 cm^3/g V_t = 0.39 cm^3/g N/C/H/O 3.07/81.28/1.12/14.53 %					q_T = 129.82 mg/g		
Wheat straw	Pyrolysis (N_2,500 °C)	S_{BET} = 38.38 m^2/g C/H/N/S/O	N_2	p-X, m-X, o-X	Flow rate: 0.2 L/min	PFOM and PSOM (which are pseudo-first and second-order	$q_{p\text{-}X}$ = 50.88 mg/g	n.d.	(Rajabi et al., 2021b)

(*continued on next page*)

Table 1 (*continued*)

Raw biosorbent	Surface modification	Biosorbent characterization	Gas matrix	Adsorbate	Adsorption conditions	Isotherm	q_{max}	Regeneration and multiple use of BS	Ref.
		66.57/2.66/0.98/ <0.3/29,49 %			$T = 25$ °C $C_0 = 100–400$ ppm_v $m_{BS} = 2$ g	models), Elovich model (ELM) Weber–Morris intra-particle diffusion model (IPDM)	$q_{m\text{-}X} = 45.37$ mg/g $q_{o\text{-}X} = 48.44$ mg/g $q_{p\text{-}X} = 25.88$ mg/g $q_{m\text{-}X} = 23.80$ mg/g $q_{o\text{-}X} = 25.32$ mg/g		
	Pyrolysis (N_2,500 °C)	$S_{BET} = 15.67$ m^2/g C/H/N/S/O 61.82/1.87/2.02/ <0.3/34.14 %		p-X, m-X, o-X					
Corn straw	Rice husks (RH)	*Trichoderma viride* pretreatment for 20 days; 600 °C carbonization (1 h), RH:KOH: 1:4 mass ratio, 800 °C activation under N_2 atmosphere (1 h)	$S_{BET} = 3714$ m^2/g $V_{mic} = 1.05$ cm^3/g $V_{mes} = 1.02$ cm^3/g $V_t = 2.04$ cm^3/g	N_2	T	Flow rate: 109 mL/min $T = 25$ °C $C_0 = 100$ ppm	Thomas model Dual-sites Langmuir-Freundlich isotherms	$q_T = 653$ mg/g	Desorption to −176 °C in N_2 atmosphere 2 cycle
(Cheng et al., 2020)									
Rice Husks (RH)	RH:KOH 1:1 mass ratio activation Pyrolysis (N_2,750 °C,4h)	$S_{BET} = 651$ m^2/g $V_{mic} = 0.26$ cm^3/g $V_{mes} = 0.16$ cm^3/g $V_t = 0.42$ cm^3/g	N_2	T	Flow rate: 30 mL/min $T = 30$ °C $C_0 = 400$ ppm $m_{BS} = 0.1$ g	Type I and IV adsorption isotherms	$q_T = 202.8$ mg/g	Programmed Desorption to 600 °C at a rate of 20 °C/min in N_2 atmosphere	(Zhang and Shen, 2019)
Defatted black cumin (*Nigella sativa* L.) biowaste	$ZnCl_2$ activation	$S_{BET} = 1213.3$ m^2/g $V_{mic} = 0.787$ cm^3/g $V_t = 0.89$ cm^3/g	N_2	B, T, X	Flow rate: 100 mL/min T = RT $C_0 = 20$ mg/L $m_{BS} = 75$ mg	Langmuir, Freundlich, and Dubinin-Radushkevich (DR)	$q_B = 495$ mg/g $q_T = 580$ mg/g $q_X = 674$ mg/g	Thermal regeneration at 140 °C in nitrogen flow	(Batur and Kutluay, 2022)
Sugarcane bagasse	Hydrothermal carbonization and KOH activation	$S_{BET} = 2455$ m^2/g $V_{mic} = 0.53$ cm^3/g $V_{mes} = 0.73$ cm^3/g $V_t = 1.26$ cm^3/g	20 % O_2 and 80 % N_2	T	V = 100 mL/min T = RT $C_0 = 1000$ ppm m = 40 mg	Bangham model	$q_T = 771.7$ mg/g	Thermal regeneration with nitrogen flow (30–450 °C, 100 mL/min) 5 cycles	(Qu et al., 2021)
Sugarcane bagasse	Urea/SB mixing weight ratio of 15 wt%, carbonization and KOH activation	$S_{BET} = 1381$ m^2/g $V_t = 0.722$ cm^3/g $V_{mic} = 0.581$ cm^3/g	20 % O_2 and 80 % N_2	T	Flow rate: 100 mL/min $T = 30$ °C $C_0 = 1000$ ppm $m_{BS} = 50$ mg	Bangham model	$q_T = 522$ mg/g	100 mL/min nitrogen gas was fed to carry the released toluene, 130 °C. toluene adsorptive capacity was only decreased by 4.5 %	(Wang et al., 2020c)
Leather solid wastes from the vegetable tanning of bovine skin	Pyrolysis and KOH activation (750 or 900 °C, N_2, 150 cm^3/min)	$S_{BET} = 2719$ m^2/g $V_{mic} = 0.829$ cm^3/g $V_t = 1.184$ cm^3/g	N_2	T	Flow rate: 250 mL/min T = RT $C_0 = 100$ ppm (384 mg/g) $m_{BS} = 250$ mg	n.d	$q_T = 27$ mg/g	Thermal regeneration (150–180 °C)	(Gil et al., 2014)
Lignocellulosic biomass (*Aesculus hippocastanum L.*)	$ZnCl_2$ 3 M activation Pyrolysis (N_2, 1200 °C)	$S_{BET} = 1858.42$ m^2/g $V_{mic} = 0.49$ cm^3/g $V_{mes} = 0.24$ cm^3/g	N_2	B,T,E, mp-X, o-X	Flow rate: 120 mL/min $T = 25$ °C $C_0 = 200$ µg/mL $m_{BS} = 0.1$ g	Langmuir Freundlich	$q_B = 844$ mg/g $q_T = 876$ µg/g $q_E = 812$ µg/g $q_{mp\text{-}X} = 1070$ µg/	–	(Isinkaralar et al., 2023)

(*continued on next page*)

Table 1 (*continued*)

Raw biosorbent	Surface modification	Biosorbent characterization	Gas matrix	Adsorbate	Adsorption conditions	Isotherm	q_{max}	Regeneration and multiple use of BS	Ref.
Hickory wood (HH)	HH: 50 % KOH 1:1 mass ratio activation Pyrolysis (N_2,600 °C)	S_{BET} = 222 m^2/g V_t = 0.050 cm^3/g 0.5–1 mm C/H/O/N 68.3/1.7/23.2/0.2	N_2	CH	Flow rate: 50 mL/min m_{BS} = 10 mg	Pseudo-first and second order model	$q_{o\text{-}X}$ = 1114 μg/g q_{CH} = 74.12 mg/g	Thermal regeneration at 150 °C in N_2 atmosphere	(Zhang et al., 2019)
	HH: 85 % H_3PO_4 1:1 mass ratio activation Pyrolysis (N_2,600 °C)	S_{BET} = 1436 m^2/g V_t = 0.028 cm^3/g V_t = 0.028 cm^3/g C/H/O/N 62.8/1.9/28.7/0.2					q_{CH} = 159.66 mg/g		
Peanut hull (PH)	PH: 50 % KOH 1:1 mass ratio activation Pyrolysis (N_2,600 °C)	S_{BET} = 571 m^2/g V_t = 0.075 cm^3/g 0.5–1 mm C/H/O/N 67.3/1.7/25.0/1.5					q_{CH} = 105.71 mg/g		
	PH: 85 % H_3PO_4 1:1 mass ratio activation Pyrolysis (N_2,600 °C)	S_{BET} = 1091 m^2/g V_t = 0.079 cm^3/g 0.5–1 mm C/H/O/N 41.5/1.7/51.6/1.1					q_{CH} = 101.04 mg/g		
Lignin-based pitch (LP)	CS:agate balls 3:200 mass ratio – 300 rpm, 5 h NH_4OH activation	S_{BET} = 405.61 m^2/g V_{mic} = 0.1844 cm^3/g V_t = 0.0384 cm^3/g C/H/O/N 70.16/2.60/15.0/2.04/0.21 % 40–100 mesh	N_2	B	Flow rate: 50 mL/min T = 25 °C V_B = 0.1369 mL $V_{m\text{-}X}$ = 0.1492 mL $V_{o\text{-}X}$ = 0.1393 mL $W_{p\text{-}X}$ = 0.1520 mL m_{BS} = 0.01 g	Pseudo-first and second order model Weber-Morris model	q_B = 119.49 mg/g $q_{m\text{-}X}$ = 128.38 mg/g $q_{o\text{-}X}$ = 121.97 mg/g $q_{p\text{-}X}$ = 130.21 mg/g	Therma desorption 130 °C in N_2 atmosphere for 6 h 4 cycles	(He et al., 2021)
Solid dealkaline lignin	Carbonization and KOH activation	S_{BET} = 2250 m^2/g V_t = 1.1 cm^3/g	N_2	B, T, Xyl	P/P_0 = 0.9 T = RT C_0 = 100 ppm	Langmuir Freundlich Sips	$q_{B,T,Xyl}$ = 600 mg/g	Thermal regeneration at 150 °C with nitrogen flow	(Saha et al., 2018)
Gasified biochar from paper mill sludge	KOH activation 2 h, 850 °C	S_{BET} = 1600 m^2/g V_t = 0.59 cm^3/g	N_2	B	Flow rate: 50 mL/min T = 25 °C C_0 = 50 ppm m_{BS} = 0.3 g	Freundlich, Dubinin–Radushkevich, Elovich fitting	q_B = 773 mg/g	Thermal regeneration at 350 °C Time 2 h 2 cycles	(Khan et al., 2019)
Asphaltene (PIA): melamine (M)	PIA:M 1:2 mass ratio KOH activation Pyrolysis (N_2, 850 °C,1 h)	S_{BET} = 2692 m^2/g V_{mic} = 0.11 cm^3/g V_{mes} = 1.61 cm^3/g V_t = 1.71 cm^3/g	N_2	B,T	T = 25 °C C_0 = 10 and 100 %	Pseudo-first order Pseudo-second order	$q_{B10\%}$ = 154.66 wt% $q_{B100\%}$ = 228.18 wt% $q_{T10\%}$ = 65.69 wt % $q_{T100\%}$ = 82.08 wt%	Thermal regeneration at 140 °C with N_2 stream at a constant flow rate of 100 mL/min	(Hossein Tehrani et al., 2020)
Volatile organochlorine compounds (VOXs)									
Coconut shell	Pyrolysis (N_2, 1173 K) Activation using HCl	S_{BET} = 1137 m^2/g V_{mic} = 0.430 cm^3/g V_t = 0.480 cm^3/g 40–60 mesh	Air	CB	Flow rate: 2 L/min T = 30 °C C_0 = 80 ppm m_{BS} = 1.2 cm^3	Langmuir Tòth Dubinin–Astakhov	q_{CB} = 255 mg/g	–	(Zhao et al., 2018)

(*continued on next page*)

Table 1 (*continued*)

Raw biosorbent	Surface modification	Biosorbent characterization	Gas matrix	Adsorbate	Adsorption conditions	Isotherm	q_{max}	Regeneration and multiple use of BS	Ref.
Lignin (sodium lignosulfonate)	Spray drying and carbonization, KOH activation	$S_{BET} = 2961\ m^2/g$ $V_t = 1.57\ cm^3/g$ $V_{mic} = 0.82\ cm^3/g$ $N = 2.34$ wt%	N_2	DCM	m = 250 mg V = 250 mL/min C_0 = 50–100 ppm	n.d.	$q_{DCM} = 156$ mg/g	Thermal regeneration at 150 °C with nitrogen flow 5 cycles	(Liu et al., 2024)
Coconut shell	Steam activation (850 °C)	$S_{BET} = 2278\ m^2/g$ $V_{mic} = 0.82\ cm^3/g$ $V_t = 1.13\ cm^3/g$ C/H/O = 93/0.6/2.5 %, wt	N_2 + H_2O	DCM TCE	V = 0.5 L/min T = 25 °C $C_0 = 0.1\ mol/m^3$ (≈2400 ppmv)	n.d.	$q_{DCM} = 2.69$ mmol/g $q_{TEM} = 6.89$ mmol/g	n.d.	(Cosnier et al., 2006)
Corn stalks (CS), rice husk (RH)	Pyrolysis (N_2, 500 °C)	$S_{BET\ (CS)} = 7.1\ m^2/g$ $S_{BET\ (RH)} = 205.4\ m^2/g$ $V_{t(CS)} = 0.016\ cm^3/g$ $V_{t(RH)} = 0.11\ cm^3/g$ $C/H/O_{(CS)}$ = 79.6/5.2/13.9 %, wt $C/H/O_{(RH)}$ = 77.2/4.5/17.7 %, wt	Air	TCE, 1,2,4-TCB, 1,2-DCB, MCB	T = 25 °C $C_{0,\ TCE} = 5.0$ mg/L $C_{0,\ 1,2,4\text{-TCB}} = 1.0$ mg/L $C_{0,\ 1,2\text{-DCB}} = 1.0$ mg/L $C_{0,\ MCB} = 1.0$ mg/L	Freundlich	$q_{TCE(CS)} = 48.4$ mg/g $q_{1,2,4\text{-TCB(CS)}} = 114.1$ mg/g $q_{1,2\text{-DCB(CS)}} = 34.1$ mg/g $q_{MCB\ (CS)} = 27.4$ mg/g $q_{TCE(RH)} = 87.4$ mg/g $q_{1,2,4\text{-TCB(RH)}} = 119.5$ mg/g $q_{1,2\text{-DCB(RH)}} = 82.8$ mg/g $q_{MCB\ (RH)} = 15.0$ mg/g Removal efficiency: BDCM = 59.9–75.7 % B = 75.8–87 % CTC = 39.6–80.6 % 1,1,1-TCM = 73.1–93.1 % CF = 52.1–77.9 % 1,1-DCE = 39.6–82.7 %	n.d.	(Han et al., 2017)
Pecan shell (PS), almond shell (AS)	Pyrolysis (N_2, 700 °C, 1 h); phosphoric acid, carbon dioxide, or steam activation	$S_{BET(AS)} = 1340\ m^2/g$ $S_{BET(PS)} = 435–917\ m^2/g$	Air	BDCM, B, CTC, 1,1,1-TCM, CF, 1,1-DCE	m = 0.01 g C_0 = 100 ppb T = 25 °C	n.d.		n.d.	(Bansode et al., 2003)
Volatile methyl siloxanes (VMSs)									
Coconut shell	Pyrolysis (N_2, 450 °C) and NaOH activation (N_2, 100 cm^3/min, 750 °C, 1 h)	$S_{BET} = 2551\ m^2/g$ $V_t = 1.3\ cm^3/g$ $V_{micro} = 1.11\ cm^3/g$ $V_{meso} = 0.2\ cm^3/g$ C/O/H/N/S = 82.8/16.1/1.01/0.08/0.03 %, wt.	Model biogas	L2	C_0 = 83.82 mg/L V = 50 mL/min T = 20 °C m = 0.25 g	Dose–response model	$q_{L2} = 898.6$ mg/g	Heating at 100 °C for 100 min; 5 regeneration cycles	(Lv et al., 2023)
Wood-Derived Char	Pyrolysis (200 kW, 450 °C)	$S_{BET} = 75.3\ m^2/g$ $V_t = 0.04\ cm^3/g$ $V_{micro} = 0.02\ cm^3/g$ $V_{meso} = 0.02\ cm^3/g$ C/K/Ca = 99.5/0.24/0.28 %, wt	CH_4:CO_2 (60:35 vol%)	D4	C_0 = 4.6–45.9 mg/m^3 T = 25 °C V = 500 mL/min	Langmuir, Freundlich, Dubinin–Radushkevich and Temkin	$q_{D4} = 4.59$ mg/m^3	n.d.	(Papurello et al., 2019)

(*continued on next page*)

Table 1 (*continued*)

Raw biosorbent	Surface modification	Biosorbent characterization	Gas matrix	Adsorbate	Adsorption conditions	Isotherm	q_{max}	Regeneration and multiple use of BS	Ref.
Coconut shell	Impregnation and calcination (N_2 60 mL/min, 600 °C, 1 h, Fe (III)-ethanol solution)	$S_{BET} = 1068.4\ m^2/g$ $V_{micro} = 0.51\ cm^3/g$	N_2	L2	m = 0.5 g T = 20 °C $C_0 = 83.82$ mg/L V = 50 mL/min	Langmuir-Freundlich model	q = 356.4 mg/g	Purging with nitrogen (100 °C, 1.5 h) and activation (100 °C, 3 h) 6 cycles	(Meng et al., 2021)
Volatile organosulfur compounds (VSCs)									
Oak	Pyrolysis (N_2, 500 °C)	$S_{BET} = 9.8\ m^2/g$	N_2	DMDS, DMTS	m = 10 g $C_{0\ (DMDS)} = 18.9$ ng/L $C_{0\ (DMTS)} = 4.8$ ng/L V = 1 L/min	Thomas model	$q_{DMDS} = 0.45$ mg/g $q_{DMTS} = 0.11$ mg/g	n.d.	(Hwang et al., 2018)
Corn starch	Carbonization (400 °C for 3 h, N_2); KOH activation (800 °C, 12 h)	$S_{BET} = 2128\ m^2/g$ $V_t = 0.89\ cm^3/g$ $V_{meso} = 0.061\ cm^3/g$ $V_{micro} = 0.81\ cm^3/g$	N_2	Methyl mercaptan (MM)	$C_0 = 0.197$ mg/L $T = 25$ °C, m = 0.1 g V = 100 mL/min	Langmuir	q = 78.16 mg/g	Purging with nitrogen (100 mL/min, 150 °C, 6 h) and chemical regeneration (20 mL of ethanol stirred for 5 h at 50 °C) 5 cycles	(Yao et al., 2022a)
Oxygenated volatile organic compounds (O-VOCs)									
Walnut shells (WS) and apricot pits (AP)	Carbonization (700 °C, N_2, 333 mL/min, 30 min); steam activation (900 °C)	$S_{BET\ (AP)} = 697\ m^2/g$ $S_{BET\ (WS)} = 686.5\ m^2/g$ H/C/S/N/O $_{(AP)}$ = 0.77/95.3/0.03/0.6/3.36 %, wt H/C/S/N/O $_{(WS)}$ = 0.81/95.6/0.03/0.423.20 %, wt	Air/H_2O	Ac	$p/p_s = 0.95$ T = 25 °C	Fritz-Schlunder model	$q_{(AP)} = 238.7$ mg/g $q_{(WS)} = 236.4$ mg/g	Vacuum pressure regeneration (10^{-6} Pa, 150 °C)	(Švábová et al., 2023)
Coconut shell activated carbon	HNO_3 activation (30 wt % HNO_3, 333 K, 2 h)	$S_{BET} = 382\ m^2/g$ $V_t = 0.228\ cm^3/g$ $V_{micro} = 0.167\ cm^3/g$	N_2	Ac	m = 200 mg $T = 300$ K. V = 250 mL/min $C_0 = 500$ ppm	n.d.	$q_{Ac} = 5.49$ mmol/g	Thermal regeneration with nitrogen flow (600 K, 10 K/min)	(Yu et al., 2018)
Coconut shell activated carbon	Acids activation (1 wt,% of H_3PO_4)	$S_{BET} = 719$ 30–35 mesh	He	MeOH, EtOH, IPA, MEK	V = 40 mL/min $T = 80$ °C $C_0 =$ 10,000–15,000 ppm $m_{BS} = 0.2$ g	Langmuir Freundlich	$q_{MeOH} = 5.65$ mmol/g $q_{EtOH} = 2.18$ mmol/g $q_{IPA} = 1.92$ mmol/g $q_{MEK} = 4$ mmol/g	Temperature programmed desorption 1 cycle	(Kim et al., 2006)
Rice husk	Carbonization (450 °C, N_2, 3 h) KOH and ball-milling activation (1000 r/min, 30 min, 750 °C, 1 h)	$S_{BET} = 1320.4\ m^2/g$ $V_t = 0.65\ cm^3/g$ $V_{micro} = 0.45\ cm^3/g$ $V_{meso} = 0.2\ cm^3/g$	N_2	Ph	V = 300 mL/min $C_0 = 31$ mg/m3 m = 0.2 g T = RT	Hybrid isotherms of type I and IV	$q_{Ac} = 1919$ mg/g	Thermal desorption (350 °C) 1 cycle	(Shen et al., 2019)
Various group of volatile organic compounds									
Hickory wood chips (HW) and peanut shell (PS)	Hydrothermal carbonization (200 °C for 6 h), CO_2 activation (150 mL/min CO_2, 2 h, 900 °C)	$S_{BET\ (HW)} = 928\ m^2/g$ $S_{BET\ (PS)} = 1308\ m^2/g$ $V_{t\ (HW)} = 0.054$	N_2	Ac, Ch	T = 20 °C m = 10 mg V = 50 mL/min $t = 1$ h.	n.d.	$q_{(HW),Ac} = 103.7$ mg/g $q_{(PS),Ac} = 122.1$ mg/g $q_{(HW),Ch} = 86.9$	Thermal desorption (150 °C, heating rate of 10 °C/min) 5 cycles	(Zhang et al., 2020)

(*continued on next page*)

Table 1 (*continued*)

Raw biosorbent	Surface modification	Biosorbent characterization	Gas matrix	Adsorbate	Adsorption conditions	Isotherm	q_{max}	Regeneration and multiple use of BS	Ref.
		cm^3/g $V_{t\ (PS)} = 0.11\ cm^3/g$ $C/H/N_{\ (HW)} = 90.5/90.5/0.4$ %, wt $C/H/N_{\ (PS)} = 86.5/2.9/2.2$ %, wt $S_{BET\ (HW)} = 1436\ m^2/g$ $S_{BET\ (PS)} = 1091\ m^2/g$					mg/g $q_{(PS),Ch} = 102.45$ mg/g		
Hickory wood chips (HW) and peanut shell (PS)	Hydrothermal carbonization (200 °C for 6 h), H_3PO_4 activation (85 % H_3PO_4, 600 °C, 1 h)	$V_{t\ (HW)} = 0.028\ cm^3/g$ $V_{t\ (PS)} = 0.079\ cm^3/g$ $C/H/O/N_{\ (HW)} = 62.8/1.9/28.7/0.2$ %, wt $C/H/O/N_{\ (PS)} = 41.5/1.7/51.6/1.1$ %, wt	N_2	Ac, Ch	T = 20 °C m = 10 mg V = 50 mL/min *t* = 1 h.	n.d.	$q_{(HW),Ac} = 148.2$ mg/g $q_{(PS),Ac} = 159.0$ mg/g $q_{(HW),Ch} = 110.5$ mg/g $q_{(PS),Ch} = 98.8$ mg/g	Thermal desorption (150 °C, heating rate of 10 °C/min) 5 cycles	(Zhang et al., 2019)
Sugarcane bagasse (BG)	Pyrolysis (N_2, 300 °C)	$S_{BET} = 5.2\ m^2/g$ C/O/H/*N* = 69.5/25.4/4.2/0.9 %, wt	N_2	Ac, Ch, T	T = RT m = 5 mg V = 50 mL/min t = 1 h C_0 = 200–220 ppmv	n.d.	$q_{Ac} = 102.4$ mg/g $q_{Ch} = 86.3$ mg/g $q_T = 65.5$ mg/g	Thermal desorption (150 °C, heating rate of 10 °C/min) 5 cycles	(Zhang et al., 2017b)
Bagasse	Pyrolysis (N_2, 500 °C)	$S_{BET} = 78.15\ m^2/g$ $V_t = 0.1448\ cm^3/g$ C/H/N/S/O = 75.94/1.77/0.40/0/21.89 %, wt	N_2	Ac, Hex, T, p-Xyl	*T* = 25 °C V = 0.2 L/min m = 2 g t = 1 h	Elovich model	$q_{Ac} = 113.0$ mg/g $q_H = 37.9$ mg/g $q_T = 46.5$ mg/g $q_{p\text{-}Xyl} = 47.1$ mg/g	Thermal desorption (95 °C, heating rate of 4.8 °C/min) 5 cycles	(Rajabi et al., 2021a)
Rice husk (RH), soft wood pellet (SW)	Pyrolysis (N_2, 550 or 700 °C)	$S_{BET(RH)} = 20.1\ m^2/g$ $S_{BET(SW)} = 162\ m^2/g$ $C/H/O/N_{(RH)} = 48.7/1.24/2.47/1.04$ %, wt $C/H/O/N_{(SW)} = 90.2/1.83/6.02/<0.1$ %, wt	N_2	MEK, B	m = 5 mg V = 330 mL min T = RT	n.d.	$q_{(RH)\ MEK} = 43$ mg/g $q_{(SW)}$ B = 2.9 mg/g	n.d.	(Vikrant et al., 2020)
Pine wood sawdust	Pyrolysis (300 °C, 3 h);	$S_{BET} = 3.76\ m^2/g$ C/O/H/*N* = 55.44/9.07/4.49/1 %, wt	N_2	Ac, T	V = 50 mL/min m = 100 mg *t* = 60 min T = RT	n.d.	$q_{Ac} = 313$ mg/g $q_T = 56$ mg/g	n.d.	(Zhuang et al., 2021)
Corn stalk (CS) and soybean straw (SS)	Pyrolysis (600 °C for 3 h) impregnation using sodium lignosulfonate (600 °C for 3 h)	$S_{BET\ (CS)} = 118.1\ m^2/g$ $V_{t(CS)} = 0.12\ cm^3/g$ $V_{micro\ (CS)} = 0.05\ cm^3/g$ $V_{meso\ (CS)} = 0.058\ cm^3/g$ $S_{BET\ (SS)} = 257.7\ m^2/g$ $V_{t(SS)} = 0.15\ cm^3/g$ $V_{micro\ (SS)} = 0.11$	N_2	Ac, B	*T* = 25 °C m = 1 g V = 50 mL/min	Langmuir and Freundlich	q_{AC} = 31.35–61.14 mg/g q_B = 44.67–80.99 mg/g	Thermal desorption (200 °C, heating rate of 10 °C/min) 10 cycles	(Zhang et al., 2022c)

(*continued on next page*)

Table 1 (*continued*)

Raw biosorbent	Surface modification	Biosorbent characterization	Gas matrix	Adsorbate	Adsorption conditions	Isotherm	q_{max}	Regeneration and multiple use of BS	Ref.
Urea-formaldehyde resins (R) and Bamboo sawdust (Bb)	Carbonization (700 °C, N_2), KOH activation (700 °C, 2 h)	cm^3/g $V_{meso\ (SS)} = 0.048$ cm^3/g $S_{BET\ (R)} = 2293.2$ m^2/g $V_{t(R)} = 1.14$ cm^3/g $V_{micro\ (R)} = 0.9$ cm^3/g $S_{BET\ (Bb)} = 1568.2$ m^2/g $V_{t(Bb)} = 0.96$ cm^3/g $V_{micro\ (Bb)} = 0.73$ cm^3/g	N_2	MeOH, T	$P = 12$ kPa $T = 25$ °C	Langmuir-Freundlich	$q_{MeOH} =$ 915.3 mg/g $q_T =$ 622.9 mg/g	n.d.	(Su et al., 2020)
Corn starch	Carbonization (400 °C for 3 h, N_2) KOH activation (800 °C, 12 h)	$S_{BET} = 2128$ m^2/g $V_t = 0.893$ cm^3/g V_{meso} 0.061 cm^3/g $V_{micro} = 0.805$ cm^3/g	N_2	Methyl mercaptan (MM), Hex, T	$C_0 =$ 30–100 ppm $C_{H2O} =$ 0 %, 30 % and 70 % T = RT	Langmuir	$q_{MM(30\%H2O)} =$ 80.2 mg/g $q_{MM(70\%H2O)} =$ 76.5 mg/g $q_{Hex(30\%H2O)} =$ 100.4 mg/g $q_{Hex(70\%H2O)} =$ 61.1 mg/g $q_{T(30\%H2O)} =$ 245.7 mg/g $q_{T(70\%H2O)} =$ 195.1 mg/g	n.d.	(Yao et al., 2022b)
Pomegranate peels	Pyrolysis (N_2, 550 °C), chemical activation KOH (20 g biochar 200 mL 3 M KOH, 1 h, 65 °C)	$S_{BET} = 8.3$ m^2/g $V_t = 0.009$ cm^3/g C/N: 67.3/O.28 %, wt	Air	DMTS, p-cresol	$C_0 = 500$ ppb_v $t = 60$ min $T = 20$ °C	Langmuir	$q_{DMTS} = 0.021$ mg/g $q_{p\text{-}cresol} = 0.013$ mg/g	Thermal desorption (100 °C, 24 h) 3 cycles	(Kaikiti et al., 2021)
Lignocellulosic waste generated in a food industry	K_2CO_3 activation (N_2 150 mL/min; 900 °C)	$S_{BET} = 1668$ m^2/g $V_t = 0.7$ cm^3/g $V_{micro} = 0.25$ cm^3/g $V_{meso} = 0.03$ cm^3/g C/H/N/S/O = 95.15/0.42/1.4/ 0.13/2.5 %, wt.	Air	L2, D4, T, Limonene	T = 25 °C m = 10–70 mg $V_{VOCs} = 4$ µL $t = 24$ h	Langmuir	$q_{L2} = 438$ mg/g $q_{D4} = 512$ mg/g $q_T = 417$ mg/g $q_{Limonene} = 446$ mg/g	n.d.	(Santos-Clotas et al., 2019)
Bamboo (Bb), sugarcane (*SC*), neem (N)	Pyrolysis (N_2, 350–550 °C)	$C/H/N/S_{(SC)} =$ 38.8/4.62/0.12/ 9.57 %, wt. $C/H/N/S_{(Bb)} =$ 42.9/6.05/0.12/ 9.57 %, wt. $C/H/N/S_{(N)} = 22.9/$ 3.16/0.31/0.18 %, wt.	N_2	B, T, Xyl, DCM, CF, CTC	V = 50 mL/min $T = 25$ °C	n.d.	$q_B =$ 1.9–54.6 mg/g $q_T =$ 13.8–65.5 mg/g $q_{DCM} =$ 9.35–39.61 mg/g $q_{Xyl} =$ 1.5–60.2 mg/g $q_{CF} =$ 9.62–30.81 mg/g $q_{CTC} =$ 9.30–40.99 mg/g	n.d.	(Kumar et al., 2020b)
Coconut shell	Carbonization (1173 K, N_2), steam activation	$S_{BET} = 1137$ m^2/g $V_t = 0.48$ cm^3/g $V_{mic} = 0.43$ cm^3/g	Air	T, CB	V = 2 L/min T = RT $C_0 = 80$ ppm $V_{BS} = 1.2$ cm^3	Yoon and Nelson and Dubinin–Astakhov	$q_{CB} = 272$ mg/g $q_T = 255$ mg/g	Thermal regeneration (167 °C, air 100 mL/min)	(Zhao et al., 2018)
Wood	Catalytic activation (NH_3·H_2O – activation	$S_{BET} = 1606.7$ m^2/g	N_2	T, DCM	$C_{0\ (DCM)} = 100$ ppm	n.d.	$q_T = 54.9$ mg/g $q_{DCM} = 308$ mg/g	n.d.	(Pi et al., 2021)

(*continued on next page*)

Table 1 (*continued*)

Raw biosorbent	Surface modification	Biosorbent characterization	Gas matrix	Adsorbate	Adsorption conditions	Isotherm	q_{max}	Regeneration and multiple use of BS	Ref.
	agent; $CaCl_2$ – catalyst, 900 °C)				$C_{0\ (T)}$ = 100 ppm V = 500 mL/min				
Hardwood alkali lignin	Carbonization (Ar,400 °C,60 min) HAL:KOH 1:4 mass ratio activation Pyrolysis (Ar,850 °C,40 min)	S_{BET} = 2587 m^2/g V_{mic} = 0.82 cm^3/g V_{mes} = 0.44 cm^3/g V_t = 1.22 cm^3/g C/O/N/S = 87.75/9.51/1.88/0.97 %, wt	N_2	DCM, T	T = 30 °C $C_{0\ (DCM)}$ = 500 ppm $C_{0\ (T)}$ = 250 ppm m = 0.1 g V = 100 mL/min	Yoon and Nelson model	q_{DCM} = 171 mg/g q_T = 518 mg/g	Thermal regeneration with nitrogen flow (30 °C) 5 cycles	(Liu et al., 2022b)
Corncob	Calcination (900 °C, 1 h, N_2) and co-activation of $(NH_4)_2C_2O_4$ and $KHCO_3$	S_{BET} = 2266 m^2/g V_t = 1.14 cm^3/g V_{mic} = 0.69 cm^3/g	N_2	B, T, CB	T = 30 °C V = 200 mL/min m = 0.05 g and 0.03 g C_0 = 300 or 500 ppm	Yoon and Nelson	q_B = 236 mg/g q_T = 547 mg/g q_{CB} = 703 mg/g	Thermal regeneration with nitrogen flow (100 mL/min, 300 °C)	(Huang et al., 2023)
Rice husk	Carbonization (N_2, 450 °C); KOH activation (N_2, 750 °C)	S_{BET} = 1818.45 m^2/g V_t = 0.9 cm^3/g V_{mic} = 0.84 cm^3/g V_{mes} = 0.11 cm^3/g	N_2	T, Ph	$V_{(T)}$ = 30 mL/min $V_{(Ph)}$ = 1 mL/min T = 20 °C $C_{0(T)}$ = 300 ppm $C_{0(Ph)}$ = 60 ppm m = 0.1 g	n.d.	q_T = 263.6 mg/g q_{Ph} = 6.53 mg/g	Thermal desorption (30–350 °C)	(Shen and Zhang, 2019)
Rapeseed cake	Carbonization (650 °C, N_2); H_2SO_4 activation	S_{BET} = 1114 m^2/g V_t = 1.47 cm^3/g	N_2	T, Ac	Flow rate: 50 mL/min T = RT C_0 = 1000 ppm m_{BS} = 15 mg	n.d.	q_T = 153,3 mg/g q_{Ac} = 148.2 mg/g	Thermal regeneration with nitrogen flow (150 °C, N_2 flow 50 mL/min)	(David, 2023)
Lignocellulosic biomass (*Aesculus hippocastanum L.*)	$ZnCl_2$ 3 M activation Pyrolysis (N_2, 1200 °C)	S_{BET} = 1858.42 m^2/g V_{mic} = 0.49 cm^3/g V_{mes} = 0.24 cm^3/g	N_2	FA	Flow rate: 120 mL/min T = 25 °C C_0 = 110 µg/m^3 m_{BS} = 0.1 g	Langmuir Freundlich	FA = 638 µg/g	–	(Isinkaralar et al., 2023)
Bamboo	$NiCl_2$-$6H_2O$ activation KOH activation Pyrolysis (N_2, 500 °C)	S_{BET} = 2181 m^2/g V_{mic} = 0.66 cm^3/g V_{mes} = 0.62 cm^3/g V_t = 1.28 cm^3/g	N_2	Mix (T,CH)	Flow rate: 150 mL/min T = 25 °C C_0 = 1000 ppm m_{BS} = 50 mg	Langmuir	q_T = 6.04 mmol/g Q_{CH} = 0.58 mmol/g q_T = 5.16 mmol/g q_{CH} = 0.54 mmol/g	Thermal regeneration at 90 °C for 2 h under a N_2 flow if 50 mL/min	(Rong et al., 2023)
Bamboo	KOH activation Pyrolysis (N_2, 500 °C)	S_{BET} = 2181 m^2/g V_{mic} = 0.66 cm^3/g V_{mes} = 0.62 cm^3/g V_t = 1.28 cm^3/g							
Wheat straw	Pyrolysis (N_2, 500 °C)	S_{BET} = 78.15 m^2/g V_t = 0.1448 cm^3/g C/H/N/O 75.94/1.77/0.40/21.89 %	N_2	Ac,H,T,p-X	Flow rate: 0.2 mL/min T = 25 °C C_0 = 200–220 ppmv m_{BS} = 0.5 ± 0.01 g	Pseudo-first and second-order models Elovich model intra-particle diffusion model	q_A = 44.50 mg/g q_H = 19.73 mg/g q_T = 32.45 mg/g $q_{p\text{-}X}$ = 51.09 mg/g q_A = 110.09 mg/g q_H = 36.82 mg/g q_T = 45.17 mg/g $q_{p\text{-}X}$ = 24.76 mg/g	Thermal regeneration at 50–60 °C 5 cycles	(Rajabi et al., 2021a)
Bagasse sugarcane		S_{BET} = 58.38 m^2/g V_t = 0.0786 cm^3/g C/H/N/S/O 66.57/2.66/0.98/<0.3/29.49 %							

activated carbon (GAC). Steam-activated pecan shell carbon demonstrated the highest total adsorption of VOCs, outperforming the coal-based commercial carbon. Additionally, the new biosorbents showed higher adsorption of 1,1,1-trichloroethane than the other carbons, indicating that pecan-and almond shell-based GACs could be effective alternatives to commercial carbon for VOCs removal (Han et al., 2017; Bansode et al., 2003).

Nitrogen-doped hierarchical porous biochar is a highly effective adsorbent for DCM removal from gas streams. A wood-based adsorbent undergoing a simple catalytic activation process and treated with NH_3-H_2O and trace amounts of $CaCl_2$ demonstrated a DCM adsorption capacity of 308 mg/g, which was higher than that of microporous biochar. This suggests that the hierarchical porosity is crucial for the simultaneous adsorption of multiple DCM molecules. The introduction of nitrogen functional groups enhances the van der Waals interactions between DCM molecules and the carbon surface, resulting in the improved combined adsorption of DCM. However, no information is available on the regeneration of biosorbents (Pi et al., 2021). Lignin-derived nitrogen-doped hierarchical porous carbon spheres produced through spray drying and carbonization-activation methods exhibited a lower adsorption capacity of 156 mg/g for DCM. Nonetheless, they maintained 86 % of their initial capacity even after undergoing five cycles of regeneration (Liu et al., 2024). The hierarchical porous activated carbon produced from alkali lignin through carbonization and activation methods demonstrated a slightly greater adsorption capacity for DCM, reaching 171 mg/g. The researchers reported that the presence of nanopores (0.5–1.0 nm) played a dominant role in the adsorption process (Liu et al., 2022b).

Kumar et al. utilized a different strategy. They discovered that thermal treatment (350–550 °C) without activation could still achieve decent adsorption efficiency. They tested the adsorption of VOCs (B, T, DCM, CF, and CTC) on biochars made from neem, sugarcane, and bamboo feedstock. The pseudo-second-order model was found to be a better fit for the experimental data than the first-order model, indicating that the adsorption of VOCs by biochar was influenced by multiple mechanisms. Although the adsorption capacity for VOCs did not exceed 40.99 mg/g, this was still a respectable result (Kumar et al., 2020b).

3.3. Volatile methyl siloxanes

Siloxanes, often referred to as volatile methyl siloxanes (VMSs), are widely used in industrial and consumer applications. However, this results in the release of VMS into the atmosphere. The two main types of volatile siloxanes are cyclic and aliphatic siloxanes. Studies have shown that VMS can accumulate in living organisms and have harmful effects on the environment. Some studies have suggested that VMS can disrupt the hormonal system, have immunosuppressive effects, and even cause cancer (Wang et al., 2020b; Pascual et al., 2021; Tran et al., 2019; Gallego et al., 2017; McBean, 2008; Piechota, 2021).

The first investigation utilized lignocellulosic waste-derived biochar without any alterations and evaluated its siloxane D4 adsorption capacity in comparison with commercial activated carbon. Despite exhibiting a significantly lower adsorption capacity (3.5 mg/g) than commercial materials (37.5 mg/g), the application of activation methods aimed at improving the physical properties of the adsorbent can anticipated to overcome this limitation (Papurello et al., 2019). Lv et al. investigated the potential of activated porous carbon (APC) derived from coconut shells to remove L2 from a gas stream. The activation process involved the use of NaOH and the coconut shells were pyrolyzed at 750 °C. This study found that the amount of NaOH used had a significant impact on the yield of L2, which can be attributed to the elimination reactions between the biosorbent and NaOH. Activation with NaOH led to the release of gases and formation of abundant micropores in the APC. However, excess NaOH promoted a strong gasification reaction that destroyed the walls between the pores and dramatically reduced the specific surface area. The obtained biosorbent had a significant specific surface area of 2551 m^2/g and a substantial total pore volume of 1.3 cm^3/g. Remarkably, at 0 °C, APC demonstrated an excellent L2 removal ability, achieving a breakthrough adsorption capacity of 898.6 mg/g. By increasing the inlet concentration of L2 and appropriately decreasing the temperature, L2 adsorption capacity can be further enhanced. One advantage of APCs is their simple recycling process, which allows for sustained adsorption performance even after five consecutive cycles of adsorption and desorption. Consequently, the prepared APC material shows great promise as an efficient adsorbent for the removal of L2 (Lv et al., 2023). In another study, lignocellulosic waste from the food and wood industries was activated with K_2CO_3 and KOH agents and used to adsorb siloxanes L2 and D4. The results were compared with those of commercial activated carbon. The adsorption capacity of the waste-derived adsorbent was similar to that of commercial activated carbon, with a range of 438–512 mg/g. The presence of narrow and numerous micropores is essential for the removal of siloxanes from biogas. The activation process at temperatures ranging from to 800–900 °C is critical for porosity development and adsorbent performance. However, these high temperatures also result in significant costs (Santos-Clotas et al., 2019). Meng et al. modified biosorbents using biochar and an Fe (III)–ethanol solution as impregnating and calcining agents, respectively. This approach required less energy for pretreatment and activation because the temperature was only 600 °C. The resulting Fe-modified biochar had a well-formed microporous structure, high specific surface area (1068.4 m^2/g) and micropore volume (0.51 cm^3/g), as well as an adsorption capacity of L2 (356.4 mg/g). However, the adsorption capacities of these materials were lower than those of NaOH-activated biosorbents because too many iron nanoparticles clogged the pores, thereby reducing the specific surface area and micropore volume (Meng et al., 2021).

3.4. Volatile oxygenates organic compounds

Oxygenated volatile organic compounds (O-VOCs) belong to the VOCs category, which are characterized by the presence of at least one oxygen atom in their molecular structure. These compounds exhibit high reactivity, mutagenicity, and potent odor, in addition to their relatively high toxicity and vapor pressure (Makoś et al., 2019; Atkinson, 2000; Beale et al., 2011; Borghoff et al., 2015; Gupta et al., 2022; Auvinen and Wirtanen, 2008; Boczkaj et al., 2016a; Li et al., 2022b).

Švábová et al. investigated the adsorption of acetone by biochars derived from walnut shells and apricot pits activated by steam or air at varying temperatures. The results showed that steam activation increased the specific surface area and acetone sorption capacity of the biochars, whereas air activation produced lower values. Additionally, pyrolysis alone led to a higher adsorption capacity for acetone than steam activation. Steam-activated biochars primarily adsorbed acetone via physical forces, whereas non-activated biochars exhibited a dual mechanism involving both physical and chemical interactions. The air-activated biosorbents displayed intermediate characteristics between these two extremes (Švábová et al., 2023). Another study on acetone adsorption utilized hydrochars from peanut shells and hickory wood chips activated with carbon dioxide. Following CO_2 activation, the specific surface area of the hydrochars increased significantly from 8 m^2/g to 1308 m^2/g, and their VOC adsorptive capacities increased from 13.24 to 24.64 mg/g to 39.42–121.74 mg/g accordingly. Investigations have revealed that polar acetone molecules interact with biosorbents via three types of intermolecular forces: induced dipole-induced dipole, dipole-induced dipole, and dipole-dipole forces (Zhang et al., 2020).

In a study conducted by Dawid, rapeseed cake (RSC) and walnut shells (WSC) were carbonized and subsequently activated with basic/acidic agents (KOH/H_2SO_4) to enhance their adsorption capabilities. The non-activated biochars showed lower adsorption capacities for acetone (26.65 mg/g), whereas the activated biochars exhibited significantly higher adsorption capacities of up to 166.7 mg/g. The biochars activated with H_2SO_4 displayed better adsorption of O-VOCs compared

to those activated with KOH (David, 2023). In another study, researchers found comparable outcomes by examining three methods of activating coconut-shell-based activated carbon with HNO_3, H_2O_2, or high heat. Activated carbon modified with HNO_3 exhibited the highest adsorption capacity of 5.49 mmol/g, which was attributed to the formation of numerous small pores and carboxylic groups on the surface of biosorbent (Yu et al., 2018). The results obtained for the other groups of O-VOCs, specifically alcohols and ketones, were also consistent. In these cases, acid activation demonstrated the highest adsorption capacity (Kim et al., 2006; Zhang et al., 2019).

The biosorbents that underwent heat treatment exhibited low acetone adsorption capacities. Specifically, the maximum adsorption capacities for bamboo (BB), sugarcane bagasse (BG), Brazilian pepper wood (BP), sugar beet tailings (BT), and hickory wood (HW) were 96.6, 102.4, 20.94, 36.4, and 58.2 mg/g, respectively, at a temperature of 300 °C (Zhang et al., 2017b). However, it should be noted that the capacity for adsorption decreased with increasing pyrolysis temperature, although the sorption area increased. For other compounds in the O-VOCs group, the same correlation can be observed (Rajabi et al., 2021a; Kaikiti et al., 2021; Vikrant et al., 2020). This phenomenon was attributed to the presence of noncarbonized organic matter in the biosorbents subjected to lower temperatures, which enabled an additional interaction known as partitioning (Zhang et al., 2017b).

Xiang et al. utilized a novel technique to activate biosorbents to remove acetone from the gas phase. They employed pyrolyzed hickory wood, which was subsequently modified via ball-milling. The ball-milled biochars exhibited improved structural properties compared to those of the pristine biochars. Specifically, they possessed a higher specific surface area (1.4–29.1 times), slightly smaller average pore size, and were more hydrophilic and polar. The ball-milled biochars also demonstrated a higher VOCs adsorption capacity (1.3–13.0 times), with a maximum acetone adsorption capacity of 103.4 mg/g. Despite this, the adsorption capacity of the ball-milled biochars was still lower than that of biosorbents activated by other methods (Xiang et al., 2020). Other types of lignocellulosic wastes, such as corn stalk, rice husk, and pine wood sawdust, were also subjected to the same modification process. However, the pyrolysis temperature used in this study was lower than that used in a previous study (300 °C). The acetone adsorption capacity achieved in this study was 304 mg/g. These findings suggest that both the choice of activation method and thermal treatment are crucial factors for enhancing the adsorption efficiency of biosorbents (Zhuang et al., 2021). Combination of various activation techniques such as ball milling and KOH activation can be employed to modify the characteristics of biomass-derived materials (Shen et al., 2019; Shen and Zhang, 2019). Using this method, the pelletized rice husks were transformed into hierarchically porous carbons with remarkable surface areas and pore volumes. These adsorbents demonstrated exceptional adsorption capabilities for phenol in the vapor phase, reaching 1919 mg/g. The high adsorption capacity was attributed to the hierarchically mesoporous structures, which facilitated the transfer of phenol molecules through the outer layer and their subsequent uptake by the adsorption sites of the inner layer sites (Shen et al., 2019).

Zheng et al. employed a less common method to impregnate corn stalk and soybean straw with sodium lignosulfonate, a natural surfactant. The biomass was then pyrolyzed and mixed with different ratios of sodium lignosulfonate. The mixture was calcined at 600 °C, and sodium lignosulfonate was used as an impregnation precursor to adjust the pore size of the biochar. The impregnated biochar was used as an adsorbent for CO_2 and VOCs, exhibiting a specific surface area and micropore volume that were 3.27 and 5.02 times higher, respectively, than those of the unimpregnated biochar. However, the VOCs adsorption capacity, particularly for acetone (80.99 mg/g), was not as satisfactory as desired (Zhang et al., 2022c).

Su et al. evaluated the methanol adsorption capacity of resin-based carbon and bamboo char through experimental and theoretical methods. Their findings revealed that N-doped porous carbon exhibited a high specific surface area, favorable microporosity, and a significant methanol adsorption capacity of 915.3 mg/g, surpassing bamboo char. The study also found that electrostatic interactions were the primary driving force behind the methanol adsorption. These results offer insights into the potential of doping with polar elements to adsorb polar gases (Su et al., 2020).

3.5. Volatile organosulfur compounds

Volatile organosulfur compounds (VOSCs) are commonly found in exhaust gases from oil refineries, pulp mills, manure and sewer systems, rayon production, wastewater treatment plants, natural and petroleum gas, and biogas generated from agri-food wastes (Varjani et al., 2020; Boczkaj et al., 2016b; Lee and Brimblecombe, 2016; De Angelis, 2012; Słupek and Makoś, 2020; Lee et al., 2006; Kasper and Feilberg, 2022). These compounds include thiols, sulfides, disulfides, and thiophenes, which have unpleasant odors even at low concentrations. The odor threshold values for VOSCs typically fall between 0.07 and 5.9 ppb (v/v). At higher concentrations (0.5 to 20 ppm, v/v), some VOSCs cause health issues such as eye irritation, dizziness, vomiting, and headaches (Andersson et al., 2004; Lomans et al., 2002; Smet et al., 1998).

This study evaluated the sorption capacities of nine biochars produced by pyrolysis of various biomass materials at different temperatures for dimethyl disulfide (DMDS) and dimethyl trisulfide (DMTS). The biochars produced from livestock manure showed low sorption capacities for both compounds, whereas those from plant biomass exhibited much higher sorption capacities. Oak biochar pyrolyzed at 500 °C had the highest sorption capacities of 0.45 and 0.11 mg/g for DMDS and DMTS, respectively, but it was only 35 % of that of commercially available activated carbon (Hwang et al., 2018). Another study explored the potential of biochar derived from pomegranate peel to remove DMTS. The biochar was produced through pyrolysis at 550 °C exhibited a high specific surface area of 8.3 m^2/g, and it is characterized by a honeycomb structure with pores and cylindrical channels, as well as increased aromaticity. This distinctive structure is responsible for the exceptional DMTS removal efficiency of nearly 99 % from the gas stream (Kaikiti et al., 2021). Yao et al. developed a new biosorbent from starch-based activated carbon, which was used to adsorb three VOCs commonly emitted by fermentation industries: MM, toluene, and n-hexane. The biosorbent had a high surface area and was rich in nitrogen and oxygen functional groups, which enhanced the adsorption of MM with a sorption capacity of 78.16 mg/g at an initial concentration of 0.197 mg/L. The biosorbent also decomposed the MM molecules into CH_3S^- and H^+, which were further adsorbed by adjacent carbon atoms containing nitrogen and oxygen functional groups (Yao et al., 2022a). The same researchers evaluated the impact of water vapor on the adsorption of MM, toluene, and n-hexane using activated carbon derived from starch in fermentation waste gas. They used the same biosorbent as that used in a previous study. The presence of water vapor in waste gas makes the adsorption of VOC gases more difficult. These results indicate that water molecules exhibit stronger adsorption energies on activated carbon than VOC molecules. At 30 % relative humidity, the water molecules displaced toluene, n-hexane, and MM from the adsorbent surface. At 70 % relative humidity, a water film formed on the adsorbent surface impeded the adsorption of n-hexane and toluene but facilitated the adsorption of MM (Yao et al., 2022b).

4. Mechanism of VOCs adsorption

The efficacy of the VOCs adsorption process using biosorbents is influenced by several factors. These parameters encompass the inherent characteristics of biosorbents, such as specific surface area, pore volume, and pore size distribution. Additionally, the quantity and nature of the active groups present on the adsorbent surface, coupled with the physicochemical attributes of the adsorbate and its concentration, significantly contribute to the overall efficiency of the process (Zhu et al.,

2020; Li et al., 2020b). The typical mechanisms of the interaction between VOCs and biosorbents are presented in Fig. 6 (Dou et al., 2011).

4.1. Pore filling

The primary mechanism of VOCs adsorption is pore filling. This mechanism relies on the porous composition of the biosorbents, encompassing specific surface areas, pore volumes, and textural properties. Based on the pore size, the pores of the adsorption material can be categorized into macropores (>50 nm), mesopores (2–50 nm), micropores (<2 nm), and narrow micropores (<1 nm) (Wei et al., 2012). The pore configuration of biodsorbents depends on both the nature of the biosorbents and their subsequent preparation. The adsorption of VOCs is influenced by the pore size distribution of the adsorbents. The effective pores accessible to VOCs are determined by the molecular diameter of the VOCs. According to the size exclusion theory, VOCs molecules can only penetrate the pores of the adsorption material if the pore diameter exceeds the molecular diameter of the VOCs. Conversely, when the pore size significantly surpasses the molecular diameter of VOCs, the adsorption force between the adsorbent and VOCs molecules becomes too weak, rendering the pore to function more as a channel (Kosuge et al., 2007). Generally, micropores serve as the primary adsorption sites, whereas mesopores facilitate the diffusion of VOCs (Li et al., 2020b). The presence of a considerable specific surface area in an biosorbents suggests enhanced adsorption abilities. This can be attributed to the larger surface area, which provides more sites for adsorption reactions, thus boosting the probability of interactions between the biosorbent and VOCs (Kim and Ahn, 2012). The size and shape of adsorbed VOCs also affects adsorption efficiency. The movement of VOC molecules through the pore channels of biosorbents is affected by steric hindrance. Smaller VOCs can easily access pores with a minimum diameter, while larger VOCs occupy pores with the maximum diameter. This demonstrates a negative linear relationship between the adsorption capacity volume of VOCs and the cross-sectional area of the molecules.

4.2. Partitioning

Partitioning is a key element in the removal of VOCs from air and industrial gases using biosorbents. During this process, VOCs permeated into the pores of the non-carbonized section. These biosorbents can readily interact with VOCs, resulting in their adsorption. However, the adsorption of VOCs is contingent on the properties of the noncarbonized part of the biosorbents (crystalline or amorphous carbon) and the carbonized crystalline and graphene fractions of the biosorbents (Chen et al., 2017). Generally, the partitioning mechanism is more pronounced and highly effective when the biosorbents have a high content of volatile matter and when the concentration of VOCs in the gas is high (Keiluweit et al., 2010). The maximum amount of non-carbonized material can be observed in biosorbents that have not undergone thermal treatment. When comparing biosorbents that have been subjected to thermal activation, significant differences in the interaction intensity can be observed owing to the pyrolysis temperature. Biosorbents that underwent pyrolysis at temperatures between 200 °C and 300 °C demonstrated the highest capacity for forming partitioning interactions. However, biosorbents pyrolyzed at lower temperatures have a very small surface area, which reduces the chances of VOCs coming into contact with the biosorbents. Consequently, only a small amount of VOCs can diffuse into biosorbents through partitioning. Therefore, even if partitioning is optimal for biosorbents produced at low pyrolysis temperatures, a large surface area is required.

4.3. Hydrogen bonding

The surfaces of biosorbents can form hydrogen bonds with many VOCs (Fang et al., 2021). These bonds involve the functional groups of both the biosorbents and organic pollutants. Biosorbents have a negative

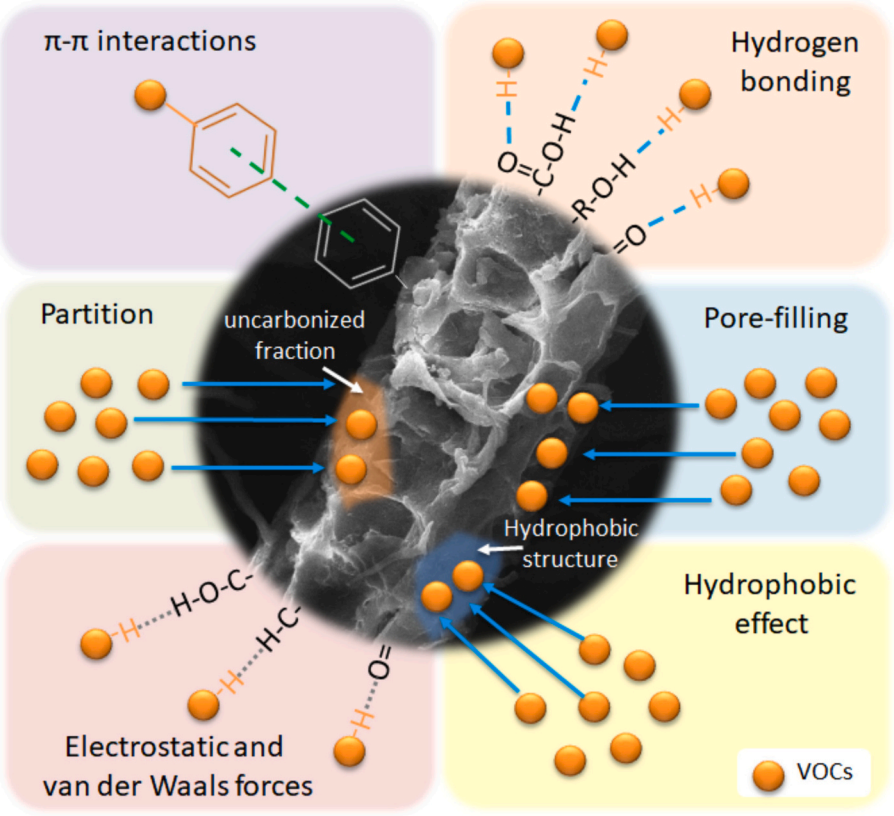

Fig. 6. Mechanisms of VOCs adsorption mechanisms into biosorbents.

charge on their surface owing to the –OH, =NH, and –NH_2 groups in unmodified plant and animal wastes (Tan et al., 2020). When biosorbents are treated with acids, they gain –COOH groups that can donate hydrogen bonds. VOCs with = O,-O-, or-O-CH_3 groups can accept hydrogen bonds and bond with biosorbents (Tan et al., 2020; Amalina et al., 2023). Biosorbents can also be doped with benzene rings and F, N, or O atoms that can accept hydrogen bonds. However, this process is irreversible because the bonds are strong (Cheng et al., 2021). This is different from most systems, in which hydrogen interactions are reversible.

4.4. Van der Waals and electrostatic interactions

The process of VOC adsorption through biosorbents is primarily driven by weak van der Waals forces, which are classified as noncovalent interactions (Zhu et al., 2020). These interactions are similar to hydrogen bonds but are significantly weaker. Van der Waals forces arise from temporary attractions between the electron-rich regions of one molecule and the electron-poor regions of another (Johnson et al., 2010). There are two types of van der Waals forces: weak London Dispersion Forces and strong dipole-dipole forces, but both are much weaker than hydrogen bonds (Tomul et al., 2021). Consequently, it is difficult to detect van der Waals forces using spectroscopic techniques.

Electrostatic interactions are a type of noncovalent interaction that differ from the other two in their long-range nature. This means that electrostatic interactions not only affect neighboring atoms, but also have an impact on atoms that are further away. These interactions are the driving forces behind the formation of ionic bonds and involve both electrostatic attraction and electrostatic repulsion. In addition, they play a significant role in the adsorption of ionizable organic compounds. These organic molecules typically exhibit affinity for negatively charged adsorbent surfaces (Rajabi et al., 2021a).

4.5. π-π and n- π interactions

π–π interactions are a form of non-covalent interactions that occur between two aromatic rings. This interaction can be observed between the aromatic rings in biosorbents and those in VOCs, such as benzene, ethylbenzene, toluene, xylene, phenol, and chlorobenzene (Jayawardhana et al., 2021; Rajabi et al., 2021b; Khan et al., 2019). This interaction is facilitated by the presence of delocalized π-electrons in the aromatic rings of both the biosorbents and VOCs. π-electrons can create a weak attractive force, leading to the adsorption of VOCs onto the surface of biosorbents. π–π interactions play a significant role in the adsorption of benzene onto biochar, contributing to the overall stability of the VOC-biosorbent complex and enhancing the efficiency of VOC removal from air or industrial gases (Jayawardhana et al., 2021). The strength and effectiveness of π–π interactions can be influenced by several factors, including the number of organic rings on the surface of the biosorbents, surface area, pore structure, and the concentration of VOCs with aromatic rings (Ahmed et al., 2018). However, the effectiveness of the π–π interaction mechanism in adsorbing VOCs onto biosorbents with weak aromatic structures is lower than that with strong aromatic structures.

Another important mechanism that can affect the adsorption of VOCs is the n–π interactions. This mechanism was first investigated by Mattson et al., who studied the donor-acceptor complex mechanism (Mattson et al., 1969). The n-pi interaction involves carbonyl oxygen, which functions as an electron donor on the biosorbent surface, and aromatic rings of VOCs, which act as electron acceptors (Tomul et al., 2021). This mechanism is essential for removing BTEX compounds by using animal-based biosorbents.

4.6. Hydrophobic interaction

Hydrophobic interactions can be harnessed for the adsorption of hydrophobic and neutral volatile organic compounds, thanks to the presence of nonpolar groups, specifically C—H bonds in molecules (Xie et al., 2020). The hydrophobic nature of biochar is a result of reduced oxygen, hydrogen, nitrogen, and sulfur content, as well as an increased carbon content due to carbonization or pyrolysis (Lin et al., 2024; Mao et al., 2019). An increase in pyrolysis temperature during biochar production leads to a decrease in polar groups, which enhances the biochar's hydrophobic characteristics (Zhang et al., 2023). The occurrence of hydrophobic interactions in biosorbents impregnated with organic substances depends on the properties of the impregnant used. The greater the hydrophobicity of the impregnant, the stronger the hydrophobic interactions between the biosorbent and hydrophobic VOCs. Additionally, compared to partitioning processes, hydrophobic interaction mechanisms require less energy (Xie et al., 2020).

5. Biosorbents regeneration and reuse

The challenge of managing various types of biosorbents is significant, both from environmental and economic standpoints. Choosing the right regeneration method is crucial, as it affects the efficiency and stability of the recycled biosorbents. Researchers have explored different techniques for regenerating adsorbents, such as temperature adjustment, pressure alteration, and gas purging (Dai et al., 2019). Thermal desorption has gained widespread acceptance owing to its efficient energy utilization and desorption performance. The process of removing VOCs from biosorbents involves three stages: The first stage is vaporization, the second stage is desorption through a multilayer mechanism, and the third stage is desorption from narrow micropores on the inner surface. Traditional adsorbents typically require high temperatures for regeneration, whereas biosorbents can be regenerated at low temperatures (Kim et al., 2006; Lv et al., 2023; Zhang et al., 2020, 2019, 2017b, 2022c; Rajabi et al., 2021a; Kaikiti et al., 2021; Shen et al., 2019; Shen and Zhang, 2019; Gil et al., 2014). However, biosorbents have the drawback of prolonged regeneration times, which can be up to 24 h (Kaikiti et al., 2021). Enhancing the process temperature can improve efficiency but can also alter the composition of the adsorbent and reduce its functionality. Thermal stability is crucial for the reusability of adsorbents, and their capacity to adsorb VOCs decreases with each regeneration cycle.

The use of inert gas to purge biosorbents is one approach to reduce the regeneration time. By passing inert gas, primarily nitrogen, through biosorbents containing adsorbed VOCs, contaminants are captured and transferred from the solid to the gas phase. This method could effectively remove all VOC groups with regeneration times not exceeding 6 h. After five adsorption-desorption cycles, no notable changes were observed in the structure of the biosorbents, and their adsorption capacities remained intact. However, it is recommended that a combination of both regeneration techniques be used for the most effective and efficient removal of VOCs from biosorbents within the shortest possible timeframe. Another approach is to reduce the pressure within the system, which alters the equilibrium conditions and causes VOCs to detach from the biosorbent material. Although this method is highly effective, it has not been extensively studied for biosorbents (Liu et al., 2024, 2022b; Meng et al., 2021; Švábová et al., 2023; David, 2023; Yu et al., 2018; Yao et al., 2022a; Saha et al., 2018; Wang et al., 2020c; Huang et al., 2023; Qu et al., 2021). The final step in biosorbent regeneration is chemical regeneration using organic solvents. This process entails removing the biosorbent from the column and transferring it to another container where an organic solvent is added. The mixture was then stirred for several hours to extract VOCs that have a higher affinity for the solvent. The solvent was then removed and the biosorbent was dried at high temperatures under an inert gas flow. This method is commonly used for regenerating biosorbents after ion adsorption; however, it is not practical for gas separation because of the complexity of the process and its high cost. Additionally, the use of organic solvents poses a significant disadvantage as they are typically toxic. Furthermore, real gas streams

may contain VOCs with different properties, making it difficult to find a solvent with high affinity for all groups of VOCs (Yao et al., 2022a; Alsawy et al., 2022).

6. Critical evaluation of biosorbents application and outlook

The use of biosorbents for treating gaseous streams has several advantages, including the ability to manage waste and high adsorptive capacity for VOCs, which often surpasses that of commercially available adsorbents. However, there are significant limitations that could hinder their implementation in industrial-scale operations, such as inconsistent reproducibility, high cost, and low yield of the preparation methods. In addition, the activation of biosorbents often requires the use of hazardous chemicals. Therefore, future research should focus on developing more environment-friendly methods for preparing and modifying biosorbents. Owing to the growing development of green solvents, that is, ionic liquids or deep eutectic solvents, which have proven effective in removing VOCs from the gas phase, new methods of biosorbent functionalization can be expected in the near future (Makoś-Chełstowska, 2023; Makoś-Chełstowska et al., 2024). Currently, bio-based waste is used to prepare sorbents and biosorbents. However, owing to increasing waste management requirements, more attention should be paid to converting non-recyclable waste (i.e., waste containing plastic) into sorbents.

A major limitation of the current understanding of VOCs adsorption using biosorbents is the lack of clarity on the mechanism, which is influenced by numerous factors that have not been adequately studied. Moreover, the authors of the present study primarily focused on the adsorption of a few VOCs from model gas streams, which may not accurately reflect real-world situations. Therefore, it is crucial that future research address this issue. Additionally, the regeneration of biosorbents presents a significant challenge because some biosorbents can only be used once, making their economic viability questionable. Furthermore, the majority of studies have only been conducted up to five adsorption-desorption cycles, which is not sufficient for real-world applications. Therefore, further research is necessary to validate the efficacy of these new sorbents. Finally, the management of biosorbents is challenging when the results of regeneration processes do not meet expectations and adsorption efficiency falls short of optimal levels. Therefore, this field requires further investigation.

Artificial Intelligence (AI) has the potential to revolutionize the production and use of biosorbents for air and industrial gas treatment. AI can analyze large datasets to identify the most suitable waste materials for biosorbent production. The yield and quality of biosorbents can be predicted based on the characteristics of different waste sources. Through machine learning algorithms, AI can optimize the conversion process, such as pyrolysis or gasification, by adjusting parameters, such as temperature, pressure, and residence time, to maximize biosorbent yield and adsorption properties. AI can assist in the functionalization of biosorbents by predicting the effects of various treatments on their surface chemistry. This includes the introduction of functional groups to enhance the ability of biochar to adsorb specific VOCs. AI systems can monitor biochar production in real time, ensure consistent quality, and identify deviations from the desired properties. This is crucial for scaling up production to an industrial level. AI can model the environmental impact of biosorbent production and use, helping to optimize the process for a minimal environmental footprint. Cost-benefit analyses can also be performed to ensure economic viability.

7. Conclusions

This review highlights the potential of agri-food waste as a biosorbent for the removal of VOCs from gas streams. This emphasizes the need to view waste as a resource for new processes, rather than as an end product. This study examines various types of waste that can be effective biosorbents, methods for their preparation, and applications in adsorbing VOCs. It also explains the key mechanisms governing the adsorption process and the importance of biosorbent regeneration for practical applications. The review concludes with a call for further research and innovation in waste management to achieve a circular economy.

Abbreviations

α	polarizability
1,1,1-TCM	1,1,1-trichloromethane
1,2,4-TCB	1,2,4-trichlorobenzene
1,1-DCM	1,1-dichloromethane
1,2-DCB	1,2-dichlorobenzene
AC	acetone
AP	apricot pits
APC	activated porous carbon
AS	almond shell
B	benzene
Bb	bamboo
BDCM	bromodichloromethane
BET	Brunauer–Emmett–Teller
BG	sugarcane bagasse
BT	sugar beet tailings
C_0	initial adsorbate concentration
CB	chlorobenzene
CF	chloroform
CH	cyclohexane
CS	Corn stalks
CTC	carbon tetrachloride
D3	hexamethylcyclopentasiloxane
D4	octamethylcyclotetrasiloxane
D5	decamethylcyclopentasiloxane
D6	dodecamethylcyclohexasiloxane
DCM	dichloromethane
DMDS	dimethyl disulfide
DMTS	dimethyl trisulfide
EEA	European Environment Agency
GAC	granular activated carbon
HW	hickory wood
L2	hexamethyldisiloxane
L3	octamethyltrisiloxane
L4	decamethyltetrasiloxane
L5	dodecamethylpentasiloxane
L-J	Lennard-Jones
m	mass of biosorbents
MCB	monochlorobenzene
MOFs	metal-organic frameworks
m-X	methyl-xylene
N	neem
O-VOCs	Oxygenated volatile organic compounds
o-X	ortho-xylene
Ph	phenol
PS	Peanut shell
p-X	para-xylene
R	Urea-formaldehyde resins
RH	rice husk
RSC	rapeseed cake
S_{BET}	total surface area
SS	soybean straw
SW	soft wood pellet
TCE	trichloroethylene
T	toluene
US EPA	United States Environmental Protection Agency
V_{meso}	mesopore volume
V_{micro}	micropore volume
V	flow rate

VMSs	Volatile methyl siloxanes
VOCs	volatile organic compounds
VOSCs	Volatile organosulfur compounds
VOXs	Volatile organochlorine compounds
V_t	total pore volume
WHO	World Health Organization
WS	walnut shells

CRediT authorship contribution statement

Patrycja Makoś-Chełstowska: Writing – review & editing, Writing – original draft, Visualization, Supervision, Project administration, Funding acquisition, Data curation, Conceptualization. **Edyta Słupek:** Writing – original draft. **Jacek Gębicki:** Writing – review & editing.

Declaration of competing interest

The authors declare that they have no known competing financial interests or personal relationships that could have appeared to influence the work reported in this paper.

Data availability

No data was used for the research described in the article.

Acknowledgments

This work was supported the National Science Centre, Poland within the grant project (No. UMO-2021/43/D/ST8/01791).

Appendix A. Supplementary data

Supplementary data to this article can be found online at https://doi.org/10.1016/j.scitotenv.2024.173910.

References

Abdullahi, A., Alhassan, M., Isah, A.G., Sani, K.A., Olalekan, O.A., 2018. Comparative studies on the kinetics of biogas purification using activated carbon and zeolite. IOP Conf. Ser. Earth Environ. Sci. 173 https://doi.org/10.1088/1755-1315/173/1/012046.

Adeniyi, A.G., Iwuozor, K.O., Emenike, E.C., Ogunniyi, S., Amoloye, M.A., Sagboye, P.A., 2023. One-step chemical activation for the production of engineered orange peel biochar. Emerg. Mater. 6, 211–221. https://doi.org/10.1007/s42247-022-00442-3.

Ahmad, W., Sethupathi, S., Munusamy, Y., Kanthasamy, R., 2021. Valorization of raw and calcined chicken eggshell for sulfur dioxide and hydrogen sulfide removal at low temperature. Catalysts 11, 1–20. https://doi.org/10.3390/catal11020295.

Ahmed, M.B., Zhou, J.L., Ngo, H.H., Johir, M.A.H., Sun, L., Asadullah, M., Belhaj, D., 2018. Sorption of hydrophobic organic contaminants on functionalized biochar: protagonist role of π-π electron-donor-acceptor interactions and hydrogen bonds. J. Hazard. Mater. 360, 270–278. https://doi.org/10.1016/J.JHAZMAT.2018.08.005.

Almohammadi, B.A., Singh, P., Sharma, S., Kumar, S., Khandelwal, B., 2021. Experimental investigation and correlation development for engine emissions with polycyclic aromatic blended formulated fuels. Fuel 303, 121280. https://doi.org/10.1016/j.fuel.2021.121280.

Almomani, F., Rene, E.R., Veiga, M.C., Bhosale, R.R., Kennes, C., 2021. Treatment of waste gas contaminated with dichloromethane using photocatalytic oxidation, biodegradation and their combinations. J. Hazard. Mater. 405, 123735 https://doi.org/10.1016/J.JHAZMAT.2020.123735.

Almomani, F.A., Bhosale, R.R., Khraisheh, M.A.M.M., Kumar, A., Kennes, C., 2018. Mineralization of dichloromethane using solar-oxidation and activated TiO2: pilot scale study. Sol. Energy 172, 116–127. https://doi.org/10.1016/J.SOLENER.2018.07.042.

Alonso-Vicario, A., Ochoa-Gómez, J.R., Gil-Río, S., Gómez-Jiménez-Aberasturi, O., Ramírez-López, C.A., Torrecilla-Soria, J., Domínguez, A., 2010. Purification and upgrading of biogas by pressure swing adsorption on synthetic and natural zeolites. Microporous Mesoporous Mater. 134, 100–107. https://doi.org/10.1016/j.micromeso.2010.05.014.

Alsawy, T., Rashad, E., El-Qelish, M., Mohammed, R.H., 2022. A comprehensive review on the chemical regeneration of biochar adsorbent for sustainable wastewater treatment. Npj Clean Water 5. https://doi.org/10.1038/s41545-022-00172-3.

Aluigi, A., Vineis, C., Tonin, C., Tonetti, C., Varesano, A., Mazzuchetti, G., 2009. Wool keratin-based nanofibres for active filtration of air and water. J. Biobaased Mater. Bioenergy 3, 311–319. https://doi.org/10.1166/jbmb.2009.1039.

Amalina, F., Krishnan, S., Zularisam, A.W., Nasrullah, M., 2023. Biochar and sustainable environmental development towards adsorptive removal of pollutants: modern advancements and future insight. Process. Saf. Environ. Prot. 173, 715–728. https://doi.org/10.1016/J.PSEP.2023.03.069.

An, H.K., Park, B.Y., Kim, D.S., 2001. Crab shell for the removal of heavy metals from aqueous solution. Water Res. 35, 3551–3556. https://doi.org/10.1016/S0043-1354(01)00099-9.

Andersson, F.A.T., Karlsson, A., Svensson, B.H., Ejlertsson, J., 2004. Occurrence and abatement of volatile sulfur compounds during biogas production. J. Air Waste Manag. Assoc. 54, 855–861. https://doi.org/10.1080/10473289.2004.10470953.

Angin, D., Altintig, E., Köse, T.E., 2013. Influence of process parameters on the surface and chemical properties of activated carbon obtained from biochar by chemical activation. Bioresour. Technol. 148, 542–549. https://doi.org/10.1016/J.BIORTECH.2013.08.164.

Atkinson, R., 2000. Atmospheric chemistry of VOCs and NOx. Atmos. Environ. 34, 2063–2101. https://doi.org/10.1016/S1352-2310(99)00460-4.

Auvinen, J., Wirtanen, L., 2008. The influence of photocatalytic interior paints on indoor air quality. Atmos. Environ. 42, 4101–4112. https://doi.org/10.1016/J.ATMOSENV.2008.01.031.

Awasthi, M.K., Sar, T., Gowd, S.C., Rajendran, K., Kumar, V., Sarsaiya, S., Li, Y., Sindhu, R., Binod, P., Zhang, Z., Pandey, A., Taherzadeh, M.J., 2023. A comprehensive review on thermochemical, and biochemical conversion methods of lignocellulosic biomass into valuable end product. Fuel 342, 127790. https://doi.org/10.1016/j.fuel.2023.127790.

Bailón, L., Nikolausz, M., Kästner, M., Veiga, M.C., Kennes, C., 2009. Removal of dichloromethane from waste gases in one- and two-liquid-phase stirred tank bioreactors and biotrickling filters. Water Res. 43, 11–20. https://doi.org/10.1016/J.WATRES.2008.09.031.

Bak, C.u., Lim, C.J., Kim, Y.D., Kim, W.S., 2019. Multi-stage adsorptive purification process for improving desulfurization performance of biogas. Sep. Purif. Technol. 227, 115702 https://doi.org/10.1016/j.seppur.2019.115702.

Baláž, M., 2018. Ball milling of eggshell waste as a green and sustainable approach: a review. Adv. Colloid Interface Sci. 256, 256–275. https://doi.org/10.1016/J.CIS.2018.04.001.

Bansode, R.R., Losso, J.N., Marshall, W.E., Rao, R.M., Portier, R.J., 2003. Adsorption of volatile organic compounds by pecan shell- and almond shell-based granular activated carbons. Bioresour. Technol. 90, 175–184. https://doi.org/10.1016/S0960-8524(03)00117-2.

Batur, E., Kutluay, S., 2022. Dynamic adsorption behavior of benzene, toluene, and xylene VOCs in single- and multi-component systems by activated carbon derived from defatted black cumin (Nigella sativa L.) biowaste. J. Environ. Chem. Eng. 10, 107565 https://doi.org/10.1016/J.JECE.2022.107565.

Beale, R., Liss, P.S., Dixon, J.L., Nightingale, P.D., 2011. Quantification of oxygenated volatile organic compounds in seawater by membrane inlet-proton transfer reaction/mass spectrometry. Anal. Chim. Acta 706, 128–134. https://doi.org/10.1016/J.ACA.2011.08.023.

Berslin, D., Reshmi, A., Sivaprakash, B., Rajamohan, N., Kumar, P.S., 2022. Remediation of emerging metal pollutants using environment friendly biochar- review on applications and mechanism. Chemosphere 290, 133384. https://doi.org/10.1016/J.CHEMOSPHERE.2021.133384.

Boczkaj, G., Makoś, P., Przyjazny, A., 2016a. Application of dynamic headspace and gas chromatography coupled to mass spectrometry (DHS-GC-MS) for the determination of oxygenated volatile organic compounds in refinery effluents. Anal. Methods 8. https://doi.org/10.1039/c5ay03043a.

Boczkaj, G., Makoś, P., Fernandes, A., Przyjazny, A., 2016b. New procedure for the control of the treatment of industrial effluents to remove volatile organosulfur compounds. J. Sep. Sci. 39 https://doi.org/10.1002/jssc.201600608.

Borghoff, S.J., Poet, T.S., Green, S., Davis, J., Hughes, B., Mensing, T., Sarang, S.S., Lynch, A.M., Hard, G.C., 2015. Methyl isobutyl ketone exposure-related increases in specific measures of α2u-globulin (α2u) nephropathy in male rats along with in vitro evidence of reversible protein binding. Toxicology 333, 1–13. https://doi.org/10.1016/J.TOX.2015.02.003.

Buekens, A., Huang, H., 1998. Comparative evaluation of techniques for controlling the formation and emission of chlorinated dioxins/furans in municipal waste incineration. J. Hazard. Mater. 62, 1–33. https://doi.org/10.1016/S0304-3894(98)00153-8.

Cabrera-Codony, A., Georgi, A., Gonzalez-Olmos, R., Valdés, H., Martín, M.J., 2017. Zeolites as recyclable adsorbents/catalysts for biogas upgrading: removal of octamethylcyclotetrasiloxane. Chem. Eng. J. 307, 820–827. https://doi.org/10.1016/j.cej.2016.09.017.

Chen, H., Gao, S., Li, Y., Xu, H.J., Li, W., Wang, J., Zhang, Y., 2022. Valorization of livestock keratin waste: application in agricultural fields. Int. J. Environ. Res. Public Health 19. https://doi.org/10.3390/ijerph19116681.

Chen, Q., Wang, Y., He, G., Yilmaz, M., Yuan, S., 2024. KMnO4-activated spinach waste biochar: An efficient adsorbent for adsorption of heavy metal ions in aqueous solution. Colloids Surfaces A Physicochem. Eng. Asp. 684, 133174 https://doi.org/10.1016/J.COLSURFA.2024.133174.

Chen, W., Yang, H., Chen, Y., Chen, X., Fang, Y., Chen, H., 2016. Biomass pyrolysis for nitrogen-containing liquid chemicals and nitrogen-doped carbon materials. J. Anal. Appl. Pyrolysis 120, 186–193. https://doi.org/10.1016/j.jaap.2016.05.004.

Chen, Y., Zhang, X., Chen, W., Yang, H., Chen, H., 2017. The structure evolution of biochar from biomass pyrolysis and its correlation with gas pollutant adsorption performance. Bioresour. Technol. 246, 101–109. https://doi.org/10.1016/j.biortech.2017.08.138.

Cheng, H., Sun, Y., Wang, X., Zou, S., Ye, G., Huang, H., Ye, D., 2020. Hierarchical porous carbon fabricated from cellulose-degrading fungus modified rice husks: ultrahigh

surface area and impressive improvement in toluene adsorption. J. Hazard. Mater. 392, 122298 https://doi.org/10.1016/j.jhazmat.2020.122298.
Cheng, N., Wang, B., Wu, P., Lee, X., Xing, Y., Chen, M., Gao, B., 2021. Adsorption of emerging contaminants from water and wastewater by modified biochar: a review. Environ. Pollut. 273, 116448 https://doi.org/10.1016/J.ENVPOL.2021.116448.
Cheng, T., Bian, Y., Li, J., Ma, X., Yang, L., Zhou, L., Wu, H., 2023. Nitrogen-doped porous biochar for selective adsorption of toluene under humid conditions. Fuel 334, 126452. https://doi.org/10.1016/j.fuel.2022.126452.
Chong, Z.T., Soh, L.S., Yong, W.F., 2023. Valorization of agriculture wastes as biosorbents for adsorption of emerging pollutants: modification, remediation and industry application. Results Eng. 17, 100960 https://doi.org/10.1016/J.RINENG.2023.100960.
Cosnier, F., Celzard, A., Furdin, G., Bégin, D., Marêché, J.F., 2006. Influence of water on the dynamic adsoprtion of chlorinated VOCs on active carbon: relative humidity of the gas phase versus pre-adsorbed water. Adsorpt. Sci. Technol. 24, 215–228. https://doi.org/10.1260/026361706778812871.
Crini, G., Lichtfouse, E., Wilson, L.D., Morin-Crini, N., 2019. Conventional and non-conventional adsorbents for wastewater treatment. Environ. Chem. Lett. 17, 195–213. https://doi.org/10.1007/s10311-018-0786-8.
Dai, Y., Zhang, N., Xing, C., Cui, Q., Sun, Q., 2019. The adsorption, regeneration and engineering applications of biochar for removal organic pollutants: a review. Chemosphere 223, 12–27. https://doi.org/10.1016/j.chemosphere.2019.01.161.
David, E., 2023. Production of activated biochar derived from residual biomass for adsorption of volatile organic compounds. Materials (Basel) 16. https://doi.org/10.3390/ma16010389.
Davidson, C.J., Hannigan, J.H., Bowen, S.E., 2021. Effects of inhaled combined benzene, toluene, ethylbenzene, and xylenes (BTEX): toward an environmental exposure model. Environ. Toxicol. Pharmacol. 81, 103518 https://doi.org/10.1016/J.ETAP.2020.103518.
De Angelis, A., 2012. Natural gas removal of hydrogen sulphide and mercaptans. Appl. Catal. Environ. 113–114, 37–42. https://doi.org/10.1016/J.APCATB.2011.11.026.
Deng, Y., Xie, Y., Zou, K., Ji, X., 2015. Review on recent advances in nitrogen-doped carbons: preparations and applications in supercapacitors. J. Mater. Chem. A 4, 1144–1173. https://doi.org/10.1039/c5ta08620e.
Dhyani, V., Bhaskar, T., 2018. A comprehensive review on the pyrolysis of lignocellulosic biomass. Renew. Energy 129, 695–716. https://doi.org/10.1016/J.RENENE.2017.04.035.
Din, M.I., Ashraf, S., Intisar, A., 2017. Comparative study of different activation treatments for the preparation of activated carbon: a mini-review. Sci. Prog. 100, 299–312. https://doi.org/10.3184/003685017X14967570531606.
Donato, R.K., Mija, A., 2020. Keratin associations with synthetic, biosynthetic and natural polymers: An extensive review. Polymers (Basel) 12, 1–64. https://doi.org/10.3390/polym12010032.
Dong, F.X., Yan, L., Zhou, X.H., Huang, S.T., Liang, J.Y., Zhang, W.X., Guo, Z.W., Guo, P. R., Qian, W., Kong, L.J., Chu, W., Diao, Z.H., 2021. Simultaneous adsorption of Cr (VI) and phenol by biochar-based iron oxide composites in water: performance, kinetics and mechanism. J. Hazard. Mater. 416, 125930 https://doi.org/10.1016/J.JHAZMAT.2021.125930.
Dou, B., Hu, Q., Li, J., Qiao, S., Hao, Z., 2011. Adsorption performance of VOCs in ordered mesoporous silicas with different pore structures and surface chemistry. J. Hazard. Mater. 186, 1615–1624. https://doi.org/10.1016/J.JHAZMAT.2010.12.051.
Durán, I., Álvarez-Gutiérrez, N., Rubiera, F., Pevida, C., 2018. Biogas purification by means of adsorption on pine sawdust-based activated carbon: impact of water vapor. Chem. Eng. J. 353, 197–207. https://doi.org/10.1016/j.cej.2018.07.100.
Elgarahy, A.M., Elwakeel, K.Z., Mohammad, S.H., Elshoubaky, G.A., 2021. A critical review of biosorption of dyes, heavy metals and metalloids from wastewater as an efficient and green process. Clean. Eng. Technol. 4, 100209 https://doi.org/10.1016/j.clet.2021.100209.
Fan, L., Ren, Y., Emmert, S., Vučković, I., Stojanovic, S., Najman, S., Schnettler, R., Barbeck, M., Schenke-Layland, K., Xiong, X., 2023. The use of collagen-based materials in bone tissue engineering. Int. J. Mol. Sci. 24 https://doi.org/10.3390/ijms24043744.
Fang, Q., Ye, S., Yang, H., Yang, K., Zhou, J., Gao, Y., Lin, Q., Tan, X., Yang, Z., 2021. Application of layered double hydroxide-biochar composites in wastewater treatment: recent trends, modification strategies, and outlook. J. Hazard. Mater. 420, 126569 https://doi.org/10.1016/j.jhazmat.2021.126569.
Feng, Y., Wu, X., Hong, N., Zhang, L., Zhang, X., Liu, Y., Zheng, H., Zhang, Q., Ruan, R., Cobb, K., 2023. Nitrogen-doped biochar from algal biomass: preparation, modification, and application. Biomass Convers. Biorefinery. https://doi.org/10.1007/s13399-023-04942-y.
Fiebig, M., Wiartalla, A., Holderbaum, B., Kiesow, S., 2014. Particulate emissions from diesel engines: correlation between engine technology and emissions. J. Occup. Med. Toxicol. 9, 1–18. https://doi.org/10.1186/1745-6673-9-6.
Funke, A., Ziegler, F., 2010. Hydrothermal carbonization of biomass: a summary and discussion of chemical mechanisms for process engineering. Biofuels Bioprod. Biorefining 4, 160–177. https://doi.org/10.1002/bbb.198.
Gaj, K., 2020. Adsorptive biogas purification from siloxanes-a critical review. Energies 13. https://doi.org/10.3390/en13102605.
Gale, M., Nguyen, T., Moreno, M., Gilliard-Abdulaziz, K.L., 2021. Physiochemical properties of biochar and activated carbon from biomass residue: influence of process conditions to adsorbent properties. ACS Omega 6, 10224–10233. https://doi.org/10.1021/acsomega.1c00530.
Gallego, E., Perales, J.F., Roca, F.J., Guardino, X., Gadea, E., 2017. Volatile methyl siloxanes (VMS) concentrations in outdoor air of several Catalan urban areas. Atmos. Environ. 155, 108–118. https://doi.org/10.1016/J.ATMOSENV.2017.02.013.
Gan, G., Fan, S., Li, X., Zhang, Z., Hao, Z., 2022. Adsorption and membrane separation for removal and recovery of volatile organic compounds. J. Environ. Sci. https://doi.org/10.1016/J.JES.2022.02.006.
Geldenhuys, G., Wattrus, M., Forbes, P.B.C., 2022. Gas and particle phase polycyclic aromatic hydrocarbon emission factors from a diesel vehicle engine: effect of operating modes in a developing country context. Atmos. Environ. X. 13, 100158 https://doi.org/10.1016/j.aeaoa.2022.100158.
Ghanbari, S., Niu, C.H., 2019. Characteristics of oat hull based biosorbent for natural gas dehydration in a PSA process. J. Nat. Gas Sci. Eng. 61, 320–332. https://doi.org/10.1016/j.jngse.2018.11.014.
Gil, M.V., Álvarez-Gutiérrez, N., Martínez, M., Rubiera, F., Pevida, C., Morán, A., 2015. Carbon adsorbents for CO2 capture from bio-hydrogen and biogas streams: breakthrough adsorption study. Chem. Eng. J. 269, 148–158. https://doi.org/10.1016/j.cej.2015.01.100.
Gil, R.R., Ruiz, B., Lozano, M.S., Martín, M.J., Fuente, E., 2014. VOCs removal by adsorption onto activated carbons from biocollagenic wastes of vegetable tanning. Chem. Eng. J. 245, 80–88. https://doi.org/10.1016/J.CEJ.2014.02.012.
Gislon, P., Galli, S., Monteleone, G., 2013. Siloxanes removal from biogas by high surface area adsorbents. Waste Manag. 33, 2687–2693. https://doi.org/10.1016/j.wasman.2013.08.023.
Gong, X., Yang, J., Feng, X., Yang, X., Zheng, H., Wu, Z., Hu, Q., 2018. Removal of thiophene in air stream by absorption combined with electrochemical oxidation. J. Taiwan Inst. Chem. Eng. 84, 173–178. https://doi.org/10.1016/J.JTICE.2018.01.022.
Grande, C.A., Rodrigues, A.E., 2007. Biogas to fuel by vacuum pressure swing adsorption I. Behavior of equilibrium and kinetic-based adsorbents. Ind. Eng. Chem. Res. 46, 4595–4605. https://doi.org/10.1021/ie061341+.
Grande, C.A., Morence, D.G.B., Bouzga, A.M., Andreassen, K.A., 2020. Silica gel as a selective adsorbent for biogas drying and upgrading. Ind. Eng. Chem. Res. 59, 10142–10149. https://doi.org/10.1021/acs.iecr.0c00949.
Gupta, M., Chaudhary, P., Singh, A., Verma, A., Yadav, D., Yadav, B.C., 2022. Development of MoO3-CdO nanoparticles based sensing device for the detection of harmful acetone levels in our skin and body via nail paint remover. Sens. Actuators B 368, 132102. https://doi.org/10.1016/J.SNB.2022.132102.
Han, L., Qian, L., Yan, J., Chen, M., 2017. Effects of the biochar aromaticity and molecular structures of the chlorinated organic compounds on the adsorption characteristics. Environ. Sci. Pollut. Res. 24, 5554–5565. https://doi.org/10.1007/s11356-016-8303-8.
He, S., Shi, G., Xiao, H., Sun, G., Shi, Y., Chen, G., Dai, H., Yuan, B., Chen, X., Yang, X., 2021. Self S-doping activated carbon derived from lignin-based pitch for removal of gaseous benzene. Chem. Eng. J. 410, 128286 https://doi.org/10.1016/j.cej.2020.128286.
Hernández, S.P., Scarpa, F., Fino, D., Conti, R., 2011. Biogas purification for MCFC application. Int. J. Hydrogen Energy 36, 8112–8118. https://doi.org/10.1016/j.ijhydene.2011.01.055.
Hossein Tehrani, N.H.M., Alivand, M.S., Rashidi, A., Rahbar Shamskar, K., Samipoorgiri, M., Esrafili, M.D., Mohammady Maklavany, D., Shafiei-Alavijeh, M., 2020. Preparation and characterization of a new waste-derived mesoporous carbon structure for ultrahigh adsorption of benzene and toluene at ambient conditions. J. Hazard. Mater. 384 https://doi.org/10.1016/j.jhazmat.2019.121317.
Hsu, C.Y., Wu, P.Y., Chen, Y.C., Chen, P.C., Guo, Y.L., Lin, Y.J., Lin, P., 2022. An integrated strategy by using long-term monitoring data to identify volatile organic compounds of high concern near petrochemical industrial parks. Sci. Total Environ. 821, 153345 https://doi.org/10.1016/J.SCITOTENV.2022.153345.
Hu, L., Cheng, W., Zhang, W., Wu, F., Peng, S., Li, J., 2017. Monolithic bamboo-based activated carbons for dynamic adsorption of toluene. J. Porous. Mater. 24, 541–549. https://doi.org/10.1007/s10934-016-0289-6.
Hu, R., Liu, G., Zhang, H., Xue, H., Wang, X., Lam, P.K.S., 2020. Odor pollution due to industrial emission of volatile organic compounds: a case study in Hefei, China. J. Clean. Prod. 246, 119075 https://doi.org/10.1016/J.JCLEPRO.2019.119075.
Hu, S.C., Chen, Y.C., Lin, X.Z., Shiue, A., Huang, P.H., Chen, Y.C., Chang, S.M., Tseng, C. H., Zhou, B., 2018. Characterization and adsorption capacity of potassium permanganate used to modify activated carbon filter media for indoor formaldehyde removal. Environ. Sci. Pollut. Res. 25, 28525–28545. https://doi.org/10.1007/s11356-018-2681-z.
Huang, X., Tang, M., Li, H., Wang, L., Lu, S., 2023. Adsorption of multicomponent VOCs on various biomass-derived hierarchical porous carbon: a study on adsorption mechanism and competitive effect. Chemosphere 313, 137513. https://doi.org/10.1016/J.CHEMOSPHERE.2022.137513.
Huang, Y., Ho, S., Lu, Y., Niu, R., Xu, L., Cao, J., Lee, S., 2016a. Removal of indoor volatile organic compounds via photocatalytic oxidation: a short review and Prospect. Molecules 21, 56. https://doi.org/10.3390/molecules21010056.
Huang, Y.F., Te Chiueh, P., Lo, S.L., 2016b. A review on microwave pyrolysis of lignocellulosic biomass, sustain. Environ. Res. 26, 103–109. https://doi.org/10.1016/j.serj.2016.04.012.
Huo, D., Zhang, X., Wei, J., Wang, J., Zhang, Q., Yang, Q., Zhu, H., Zhang, F., Fang, G., Wu, T., 2024. Preparation and characterization of cellulose nanofibril/chitosan aerogels with high-adsorbability and sensitive indication for indoor free formaldehyde. Int. J. Biol. Macromol. 259, 128891 https://doi.org/10.1016/J.IJBIOMAC.2023.128891.
Hwang, O., Lee, S.R., Cho, S., Ro, K.S., Spiehs, M., Woodbury, B., Silva, P.J., Han, D.W., Choi, H., Kim, K.Y., Jung, M.W., 2018. Efficacy of different biochars in removing odorous volatile organic compounds (VOCs) emitted from swine manure. ACS Sustain. Chem. Eng. 6, 14239–14247. https://doi.org/10.1021/acssuschemeng.8b02881.

Irvan, B. Trisakti, Maulina, S., Sidabutar, R., Iriany, M.S. Takriff, 2018. Adsorption - desorption system for co 2 removal in biogas using natural zeolite - based adsorbent. J. Eng. Sci. Technol. 13, 3058–3070.
Isinkaralar, K., Gullu, G., Turkyilmaz, A., 2023. Experimental study of formaldehyde and BTEX adsorption onto activated carbon from lignocellulosic biomass. Biomass Convers. Biorefinery. 13, 4279–4289. https://doi.org/10.1007/s13399-021-02287-y.
Ivanovski, M., Goricanec, D., Krope, J., Urbancl, D., 2022. Torrefaction pretreatment of lignocellulosic biomass for sustainable solid biofuel production. Energy 240, 122483. https://doi.org/10.1016/J.ENERGY.2021.122483.
Jayawardhana, Y., Keerthanan, S., Lam, S.S., Vithanage, M., 2021. Ethylbenzene and toluene interactions with biochar from municipal solid waste in single and dual systems. Environ. Res. 197, 111102 https://doi.org/10.1016/j.envres.2021.111102.
Jiang, H., Ye, Y., Lu, P., Zhao, M., Xu, G., Chen, D., Song, T., 2021. Effects of torrefaction conditions on the hygroscopicity of biochars. J. Energy Inst. 96, 260–268. https://doi.org/10.1016/J.JOEI.2021.03.018.
Jimenez-Cordero, D., Heras, F., Alonso-Morales, N., Gilarranz, M.A., Rodriguez, J.J., 2015. Ozone as oxidation agent in cyclic activation of biochar. Fuel Process. Technol. 139, 42–48. https://doi.org/10.1016/J.FUPROC.2015.08.016.
Johnson, E.R., Keinan, S., Mori-Sánchez, P., Contreras-García, J., Cohen, A.J., Yang, W., 2010. Revealing noncovalent interactions. J. Am. Chem. Soc. 132, 6498–6506. https://doi.org/10.1021/ja100936w.
Jung, S., Park, Y.K., Kwon, E.E., 2019. Strategic use of biochar for CO2 capture and sequestration. J. CO2 Util. 32, 128–139. https://doi.org/10.1016/j.jcou.2019.04.012.
Kaikiti, K., Stylianou, M., Agapiou, A., 2021. Development of food-origin biochars for the adsorption of selected volatile organic compounds (VOCs) for environmental matrices. Bioresour. Technol. 342, 125881 https://doi.org/10.1016/j.biortech.2021.125881.
Kan, T., Strezov, V., Evans, T.J., 2016. Lignocellulosic biomass pyrolysis: a review of product properties and effects of pyrolysis parameters. Renew. Sustain. Energy Rev. 57, 1126–1140. https://doi.org/10.1016/j.rser.2015.12.185.
Karić, N., Maia, A.S., Teodorović, A., Atanasova, N., Langergraber, G., Crini, G., Ribeiro, A.R.L., Đolić, M., 2022. Bio-waste valorisation: agricultural wastes as biosorbents for removal of (in)organic pollutants in wastewater treatment. Chem. Eng. J. Adv. 9, 100239 https://doi.org/10.1016/J.CEJA.2021.100239.
Kasera, N., Kolar, P., Hall, S.G., 2022. Nitrogen-doped biochars as adsorbents for mitigation of heavy metals and organics from water: a review. Biochar 4. https://doi.org/10.1007/s42773-022-00145-2.
Kasper, P.L., Feilberg, A., 2022. Regenerative one-stage catalytic absorption process with cupric ions for removal of reduced sulfur compounds in polluted air. Environ. Technol. 1–11. https://doi.org/10.1080/09593330.2022.2077132 (United Kingdom).
Keiluweit, M., Nico, P.S., Johnson, M., Kleber, M., 2010. Dynamic molecular structure of plant biomass-derived black carbon (biochar). Environ. Sci. Technol. 44, 1247–1253. https://doi.org/10.1021/es9031419.
Khan, A., Szulejko, J.E., Samaddar, P., Kim, K.H., Liu, B., Maitlo, H.A., Yang, X., Ok, Y.S., 2019. The potential of biochar as sorptive media for removal of hazardous benzene in air. Chem. Eng. J. 361, 1576–1585. https://doi.org/10.1016/j.cej.2018.10.193.
Khan, A.A., Ahmad, I., Ahmad, R., 2020. Influence of electric field on CO2 removal by P-doped C60-fullerene: a DFT study. Chem. Phys. Lett. 742, 137155 https://doi.org/10.1016/J.CPLETT.2020.137155.
Khan, F.I., Kr, A., 2000. Ghoshal, removal of volatile organic compounds from polluted air. J. Loss Prev. Process Ind. 13, 527–545. https://doi.org/10.1016/S0950-4230(00)00007-3.
Khosa, M.A., Wu, J., Ullah, A., 2013. Chemical modification, characterization, and application of chicken feathers as novel biosorbents. RSC Adv. 3, 20800–20810. https://doi.org/10.1039/c3ra43787f.
Kiciński, W., Szala, M., Bystrzejewski, M., 2014. Sulfur-doped porous carbons: synthesis and applications. Carbon N. Y. 68, 1–32. https://doi.org/10.1016/J.CARBON.2013.11.004.
Kim, K.J., Ahn, H.G., 2010. The adsorption and desorption characteristics of a binary component system of toluene and methylethylketone on activated carbon modified with phosphoric acid. Carbon N. Y. 48, 2198–2202. https://doi.org/10.1016/j.carbon.2010.02.021.
Kim, K.J., Ahn, H.G., 2012. The effect of pore structure of zeolite on the adsorption of VOCs and their desorption properties by microwave heating. Microporous Mesoporous Mater. 152, 78–83. https://doi.org/10.1016/J.MICROMESO.2011.11.051.
Kim, K.J., Kang, C.S., You, Y.J., Chung, M.C., Woo, M.W., Jeong, W.J., Park, N.C., Ahn, H.G., 2006. Adsorption-desorption characteristics of VOCs over impregnated activated carbons. Catal. Today 111, 223–228. https://doi.org/10.1016/j.cattod.2005.10.030.
Kosuge, K., Kubo, S., Kikukawa, N., Takemori, M., 2007. Effect of pore structure in mesoporous silicas on VOC dynamic adsorption/desorption performance. Langmuir 23, 3095–3102. https://doi.org/10.1021/la062616t.
Kumar, A., Singh, E., Khapre, A., Bordoloi, N., Kumar, S., 2020b. Sorption of volatile organic compounds on non-activated biochar. Bioresour. Technol. 297, 122469 https://doi.org/10.1016/j.biortech.2019.122469.
Kumar, V., Kumar, S., Kim, K.H., Tsang, D.C.W., Lee, S.S., 2019. Metal organic frameworks as potent treatment media for odorants and volatiles in air. Environ. Res. 168, 336–356. https://doi.org/10.1016/j.envres.2018.10.002.
Kumar, V., Lee, Y.S., Shin, J.W., Kim, K.H., Kukkar, D., Fai Tsang, Y., 2020a. Potential applications of graphene-based nanomaterials as adsorbent for removal of volatile organic compounds. Environ. Int. 135, 105356 https://doi.org/10.1016/j.envint.2019.105356.
Kuranchie, F.A., Angnunavuri, P.N., Attiogbe, F., Nerquaye-Tetteh, E.N., 2019. Occupational exposure of benzene, toluene, ethylbenzene and xylene (BTEX) to pump attendants in Ghana: implications for policy guidance. Cogent Environ. Sci. 5 https://doi.org/10.1080/23311843.2019.1603418.
Kusrini, E., Wu, S., Susanto, B.H., Lukita, M., Gozan, M., Hans, M.D., Rahman, A., Degirmenci, V., Usman, A., 2019. Simultaneous absorption and adsorption processes for biogas purification using Ca(OH)2 solution and activated clinoptilolite zeolite/chitosan composites. Int. J. Technol. 10, 1243–1250. https://doi.org/10.14716/ijtech.v10i6.3695.
Kutluay, S., Baytar, O., Şahin, Ö., 2019. Equilibrium, kinetic and thermodynamic studies for dynamic adsorption of benzene in gas phase onto activated carbon produced from elaeagnus angustifolia seeds. J. Environ. Chem. Eng. 7 https://doi.org/10.1016/j.jece.2019.102947.
Kwaśny, J., Balcerzak, W., 2016. Sorbents used for biogas desulfurization in the adsorption process. Polish J. Environ. Stud. 25, 37–43. https://doi.org/10.15244/pjoes/60259.
Lee, C.L., Brimblecombe, P., 2016. Anthropogenic contributions to global carbonyl sulfide, carbon disulfide and organosulfides fluxes. Earth-Science Rev. 160, 1–18. https://doi.org/10.1016/J.EARSCIREV.2016.06.005.
Lee, S., Xu, Q., Booth, M., Townsend, T.G., Chadik, P., Bitton, G., 2006. Reduced sulfur compounds in gas from construction and demolition debris landfills. Waste Manag. 26, 526–533. https://doi.org/10.1016/J.WASMAN.2005.10.010.
Li, C., He, L., Yao, X., Yao, Z., 2022a. Recent advances in the chemical oxidation of gaseous volatile organic compounds (VOCs) in liquid phase. Chemosphere 295, 133868. https://doi.org/10.1016/J.CHEMOSPHERE.2022.133868.
Li, L., Liu, S., Liu, J., 2011. Surface modification of coconut shell based activated carbon for the improvement of hydrophobic VOC removal. J. Hazard. Mater. 192, 683–690. https://doi.org/10.1016/j.jhazmat.2011.05.069.
Li, W., Lu, H.T., Doblin, M.S., Bacic, A., Stevens, G.W., Mumford, K.A., 2022b. A solvent loss study for the application of solvent extraction processes in the pharmaceutical industry. Chem. Eng. Sci. 250, 117400 https://doi.org/10.1016/J.CES.2021.117400.
Li, X., Zhang, L., Yang, Z., Wang, P., Yan, Y., Ran, J., 2020b. Adsorption materials for volatile organic compounds (VOCs) and the key factors for VOCs adsorption process: a review. Sep. Purif. Technol. 235, 116213 https://doi.org/10.1016/J.SEPPUR.2019.116213.
Li, Z., Yang, D.P., Chen, Y., Du, Z., Guo, Y., Huang, J., Li, Q., 2020a. Waste eggshells to valuable Co3O4/CaCO3 materials as efficient catalysts for VOCs oxidation. Mol. Catal. 483, 110766 https://doi.org/10.1016/J.MCAT.2020.110766.
Liang, C., Gascó, G., Fu, S., Méndez, A., Paz-Ferreiro, J., 2016. Biochar from pruning residues as a soil amendment: effects of pyrolysis temperature and particle size. Soil Tillage Res. 164, 3–10. https://doi.org/10.1016/j.still.2015.10.002.
Liang, Z., Wang, J., Zhang, Y., Han, C., Ma, S., Chen, J., Li, G., An, T., 2020. Removal of volatile organic compounds (VOCs) emitted from a textile dyeing wastewater treatment plant and the attenuation of respiratory health risks using a pilot-scale biofilter. J. Clean. Prod. 253, 120019 https://doi.org/10.1016/J.JCLEPRO.2020.120019.
Lin, J., Xu, Z., Zhang, Q., Cao, Y., Mašek, O., Lei, H., Tsang, D.C.W., 2024. Enhanced adsorption of aromatic VOCs on hydrophobic porous biochar produced via microwave rapid pyrolysis. Bioresour. Technol. 393, 130085 https://doi.org/10.1016/J.BIORTECH.2023.130085.
Liu, C., Zhang, H., Xiao, R., Wu, S., 2017a. Value-added organonitrogen chemicals evolution from the pyrolysis of chitin and chitosan. Carbohydr. Polym. 156, 118–124. https://doi.org/10.1016/j.carbpol.2016.09.024.
Liu, C., Xin, Y., Zhang, C., Liu, J., Liu, P., He, X., Mu, Y., 2022a. Ambient volatile organic compounds in urban and industrial regions in Beijing: characteristics, source apportionment, secondary transformation and health risk assessment. Sci. Total Environ., 158873 https://doi.org/10.1016/J.SCITOTENV.2022.158873.
Liu, S., Cai, Y., Zhao, X., Liang, Y., Zheng, M., Hu, H., Dong, H., Jiang, S., Liu, Y., Xiao, Y., 2017b. Sulfur-doped nanoporous carbon spheres with ultrahigh specific surface area and high electrochemical activity for supercapacitor. J. Power Sources 360, 373–382. https://doi.org/10.1016/J.JPOWSOUR.2017.06.029.
Liu, S., Wei, W., Wu, S., Zhang, F., Cheng, H., 2022b. Efficient dichloromethane and toluene removal via lignin derived oxygen and nitrogen-containing activated carbons with well-developed micro-mesopore structure. Diamond Relat. Mater. 124, 108922 https://doi.org/10.1016/J.DIAMOND.2022.108922.
Liu, S., Wu, S., Li, M., Li, Y., Wang, X., 2024. Lignin-derived nitrogen doped hierarchical porous carbon spheres for highly efficient dichloromethane adsorption. Ind. Crop. Prod. 209, 118053 https://doi.org/10.1016/J.INDCROP.2024.118053.
Lomans, B.P., Van Der Drift, C., Pol, A., Den Camp, H.J.M.O., 2002. Microbial cycling of volatile organic sulfur compounds. Cell. Mol. Life Sci. 59, 575–588.
Lu, H., Xu, G., Gan, L., 2022b. N doped activated biochar from Pyrolyzing wood powder for prompt BPA removal via Peroxymonosulfate activation. Catalysts 12. https://doi.org/10.3390/catal12111449.
Lu, Y., Pang, X., Lyu, Y., Li, J., Xing, B., Chen, J., Mao, Y., Shang, Q., Wu, H., 2022a. Characteristics and sources analysis of ambient volatile organic compounds in a typical industrial park: implications for ozone formation in 2022 Asian Games. Sci. Total Environ. 848, 157746 https://doi.org/10.1016/J.SCITOTENV.2022.157746.
Lv, S., Ma, X., Fu, Q., Zheng, Y., Ma, Z., 2023. Removal of hexamethyldisiloxane by NaOH–activated porous carbons produced from coconut shells. Catalysts 13, 1–12. https://doi.org/10.3390/catal13060918.
Lyu, H., Xia, S., Tang, J., Zhang, Y., Gao, B., Shen, B., 2020. Thiol-modified biochar synthesized by a facile ball-milling method for enhanced sorption of inorganic Hg2+ and organic CH3Hg+. J. Hazard. Mater. 384, 121357 https://doi.org/10.1016/J.JHAZMAT.2019.121357.

Makoś, P., Przyjazny, A., Boczkaj, G., 2019. Methods of assaying volatile oxygenated organic compounds in effluent samples by gas chromatography—a review. J. Chromatogr. A 1592, 143–160. https://doi.org/10.1016/j.chroma.2019.01.045.
Makoś, P., Słupek, E., Małachowska, A., 2020. Silica gel impregnated by deep eutectic solvents for adsorptive removal of BTEX from gas streams. Materials (Basel) 13, 1894. https://doi.org/10.3390/ma13081894.
Makoś-Chełstowska, P., 2023. VOCs absorption from gas streams using deep eutectic solvents – a review. J. Hazard. Mater. 448, 130957 https://doi.org/10.1016/j.jhazmat.2023.130957.
Makoś-Chełstowska, P., Słupek, E., Gębicki, J., 2021. Deep eutectic solvent-based green absorbents for the effective removal of volatile organochlorine compounds from biogas. Green Chem. 4814–4827. https://doi.org/10.1039/d1gc01735g.
Makoś-Chełstowska, P., Sikorska, D., Janicka, P., Słupek, E., Mielewczyk-Gryń, A., Gębicki, J., 2024. Lignocellulosic waste biosorbents infused with deep eutectic solvents for biogas desulfurization. Chem. Eng. J. 493, 152639 https://doi.org/10.1016/J.CEJ.2024.152639.
Mallah, M.A., Changxing, L., Mallah, M.A., Noreen, S., Liu, Y., Saeed, M., Xi, H., Ahmed, B., Feng, F., Mirjat, A.A., Wang, W., Jabar, A., Naveed, M., Li, J.H., Zhang, Q., 2022. Polycyclic aromatic hydrocarbon and its effects on human health: an overeview. Chemosphere 296. https://doi.org/10.1016/j.chemosphere.2022.133948.
Mao, J., Zhang, K., Chen, B., 2019. Linking hydrophobicity of biochar to the water repellency and water holding capacity of biochar-amended soil. Environ. Pollut. 253, 779–789. https://doi.org/10.1016/J.ENVPOL.2019.07.051.
Martínez De Yuso, A., Izquierdo, M.T., Rubio, B., Carrott, P.J.M., 2013. Adsorption of toluene and toluene-water vapor mixture on almond shell based activated carbons. Adsorption 19, 1137–1148. https://doi.org/10.1007/s10450-013-9540-5.
Mattson, J.A., Mark, H.B., Malbin, M.D., Weber, W.J., Crittenden, J.C., 1969. Surface chemistry of active carbon: specific adsorption of phenols. J. Colloid Interface Sci. 31, 116–130. https://doi.org/10.1016/0021-9797(69)90089-7.
McBean, E.A., 2008. Siloxanes in biogases from landfills and wastewater digesters. Can. J. Civ. Eng. 35, 431–436. https://doi.org/10.1139/L07-144.
M. Meena, P. Sonigra, G. Yadav, Biological-based methods for the removal of volatile organic compounds (VOCs) and heavy metals, (n.d.). doi:https://doi.org/10.1007/s11356-020-11112-4/Published.
Meng, Z., Liu, Y., Li, X., Ma, Z., 2020. Removal of siloxane (L2) from biogas using methyl-functionalised silica gel as adsorbent. Chem. Eng. J. 389, 124440 https://doi.org/10.1016/j.cej.2020.124440.
Meng, Z., Hou, X., Liu, Y., Ma, Z., Shen, H., 2021. Facile fabrication of iron-modified biochar as a renewable adsorbent for efficient siloxane (L2) removal. J. Environ. Chem. Eng. 9, 105799 https://doi.org/10.1016/j.jece.2021.105799.
Mohamad Nor, N., Lau, L.C., Lee, K.T., Mohamed, A.R., 2013. Synthesis of activated carbon from lignocellulosic biomass and its applications in air pollution control - a review. J. Environ. Chem. Eng. 1, 658–666. https://doi.org/10.1016/j.jece.2013.09.017.
Mohamed, M., Ouki, S.K., 2011. Kinetic and removal mechanisms of ethylbenzene from contaminated solutions by chitin and chitosan. Water Air Soil Pollut. 220, 131–140. https://doi.org/10.1007/s11270-010-0740-2.
Mohammed, J., Nasri, N.S., Ahmad Zaini, M.A., Hamza, U.D., Ani, F.N., 2015. Adsorption of benzene and toluene onto KOH activated coconut shell based carbon treated with NH3. Int. Biodeterior. Biodegrad. 102, 245–255. https://doi.org/10.1016/j.ibiod.2015.02.012.
Mosleh, M.H., Rajabi, H., 2024. NaOH-benzoic acid modified biochar for enhanced removal of aromatic VOCs. Sep. Purif. Technol. 330, 125453 https://doi.org/10.1016/j.seppur.2023.125453.
Mu, M., Zhang, X., Yu, G., Sun, C., Xu, R., Liu, N., Wang, N., Chen, B., Dai, C., 2022. Deep removal of chlorobenzene based volatile organic compounds from exhaust gas with ionic liquids. Sep. Purif. Technol. 298, 121610 https://doi.org/10.1016/J.SEPPUR.2022.121610.
N, Y.K., T, P.D., P, S., S, K., Ra, Y.K., Varjani, S., AdishKumar, S., Kumar, G., J, R.B., 2022. Lignocellulosic biomass-based pyrolysis: a comprehensive review. Chemosphere 286, 131824. https://doi.org/10.1016/J.CHEMOSPHERE.2021.131824.
Niu, J., Shao, R., Liu, M., Zan, Y., Dou, M., Liu, J., Zhang, Z., Huang, Y., Wang, F., 2019. Porous carbons derived from collagen-enriched biomass: tailored design, synthesis, and application in electrochemical energy storage and conversion. Adv. Funct. Mater. 29, 1–23. https://doi.org/10.1002/adfm.201905095.
Ong, H.C., Yu, K.L., Chen, W.H., Pillejera, M.K., Bi, X., Tran, K.Q., Pétrissans, A., Pétrissans, M., 2021. Variation of lignocellulosic biomass structure from torrefaction: a critical review. Renew. Sustain. Energy Rev. 152 https://doi.org/10.1016/j.rser.2021.111698.
Palniandy, L.K., Yoon, L.W., Wong, W.Y., Yong, S.T., Pang, M.M., 2019. Application of biochar derived from different types of biomass and treatment methods as a fuel source for direct carbon fuel cells. Energies 12, 1–15. https://doi.org/10.3390/en12132477.
Panwar, N.L., Pawar, A., 2022. Influence of activation conditions on the physicochemical properties of activated biochar: a review. Biomass Convers. Biorefinery. 12, 925–947. https://doi.org/10.1007/s13399-020-00870-3.
Papurello, D., Gandiglio, M., Kafashan, J., Lanzini, A., 2019. Biogas purification: a comparison of adsorption wood-derived char using isotherm equations. Processes 7, 774.
Pascual, C., Cantera, S., Lebrero, R., 2021. Volatile siloxanes emissions: impact and sustainable abatement perspectives. Trends Biotechnol. 39, 1245–1248. https://doi.org/10.1016/J.TIBTECH.2021.05.003.
Peluso, A., Gargiulo, N., Aprea, P., Pepe, F., Caputo, D., 2019. Nanoporous materials as H2S adsorbents for biogas purification: a review. Sep. Purif. Rev. 48, 78–89. https://doi.org/10.1080/15422119.2018.1476978.
Peter, S., Lyczko, N., Gopakumar, D., Maria, H.J., Nzihou, A., Thomas, S., 2021. Chitin and chitosan based composites for energy and environmental applications: a review. Waste Biomass Valoriz. 12, 4777–4804. https://doi.org/10.1007/s12649-020-01244-6.
Pi, X., Qu, Z., Sun, F., Zhang, Z., Gao, J., 2021. Catalytic activation preparation of nitrogen-doped hierarchical porous bio-char for efficient adsorption of dichloromethane and toluene. J. Anal. Appl. Pyrolysis 156, 105150. https://doi.org/10.1016/J.JAAP.2021.105150.
Piechota, G., 2021. Removal of siloxanes from biogas upgraded to biomethane by cryogenic temperature condensation system. J. Clean. Prod. 308, 127404 https://doi.org/10.1016/J.JCLEPRO.2021.127404.
Premchand, P., Demichelis, F., Chiaramonti, D., Bensaid, S., Fino, D., 2023. Biochar production from slow pyrolysis of biomass under CO2 atmosphere: a review on the effect of CO2 medium on biochar production, characterisation, and environmental applications. J. Environ. Chem. Eng. 11, 110009 https://doi.org/10.1016/j.jece.2023.110009.
Qin, H., Hu, T., Zhai, Y., Lu, N., Aliyeva, J., 2020. The improved methods of heavy metals removal by biosorbents: a review. Environ. Pollut. 258, 113777 https://doi.org/10.1016/j.envpol.2019.113777.
Qiu, B., Shao, Q., Shi, J., Yang, C., Chu, H., 2022. Application of biochar for the adsorption of organic pollutants from wastewater: modification strategies, mechanisms and challenges. Sep. Purif. Technol. 300, 121925 https://doi.org/10.1016/J.SEPPUR.2022.121925.
Qu, Y., Xu, L., Chen, Y., Sun, S., Wang, Y., Guo, L., 2021. Efficient toluene adsorption/desorption on biochar derived from in situ acid-treated sugarcane bagasse 62616–62627.
Rajabi, H., Hadi Mosleh, M., Prakoso, T., Ghaemi, N., Mandal, P., Lea-Langton, A., Sedighi, M., 2021a. Competitive adsorption of multicomponent volatile organic compounds on biochar. Chemosphere 283, 131288. https://doi.org/10.1016/j.chemosphere.2021.131288.
Rajabi, H., Mosleh, M.H., Mandal, P., Lea-Langton, A., Sedighi, M., 2021b. Sorption behaviour of xylene isomers on biochar from a range of feedstock. Chemosphere 268, 129310. https://doi.org/10.1016/j.chemosphere.2020.129310.
Rong, Y., Pan, C., Song, K., Chol Nam, J., Wu, F., You, Z., Hao, Z., Li, J., Zhang, Z., 2023. Bamboo-derived hydrophobic porous graphitized carbon for adsorption of volatile organic compounds. Chem. Eng. J. 461, 141979 https://doi.org/10.1016/j.cej.2023.141979.
Saha, D., Mirando, N., Levchenko, A., 2018. Liquid and vapor phase adsorption of BTX in lignin derived activated carbon: equilibrium and kinetics study. J. Clean. Prod. 182, 372–378. https://doi.org/10.1016/J.JCLEPRO.2018.02.076.
Sajjadi, B., Chen, W.Y., Egiebor, N.O., 2019. A comprehensive review on physical activation of biochar for energy and environmental applications. Rev. Chem. Eng. 35, 735–776. https://doi.org/10.1515/revce-2017-0113.
Sakhiya, A.K., Anand, A., Kaushal, P., 2020. Production, activation, and applications of biochar in recent times. Springer Singapore. https://doi.org/10.1007/s42773-020-00047-1.
Salazar Gómez, J.I., Lohmann, H., Krassowski, J., 2016. Determination of volatile organic compounds from biowaste and co-fermentation biogas plants by single-sorbent adsorption. Chemosphere 153, 48–57. https://doi.org/10.1016/J.CHEMOSPHERE.2016.02.128.
Salindeho, N., Mokolensang, J.F., Manu, L., Taslim, N.A., Nurkolis, F., Ben Gunawan, W., Yusuf, M., Mayulu, N., Tsopmo, A., 2022. Fish scale rich in functional compounds and peptides: a potential nutraceutical to overcome undernutrition. Front. Nutr. 9 https://doi.org/10.3389/fnut.2022.1072370.
Santos-Clotas, E., Cabrera-Codony, A., Ruiz, B., Fuente, E., Martín, M.J., 2019. Sewage biogas efficient purification by means of lignocellulosic waste-based activated carbons. Bioresour. Technol. 275, 207–215. https://doi.org/10.1016/j.biortech.2018.12.060.
Sarker, T.R., Nanda, S., Dalai, A.K., Meda, V., 2021. A review of torrefaction technology for upgrading lignocellulosic biomass to solid biofuels. Bioenergy Res. 14, 645–669. https://doi.org/10.1007/s12155-020-10236-2.
Shen, Y., Zhang, N., 2019. Facile synthesis of porous carbons from silica-rich rice husk char for volatile organic compounds (VOCs) sorption. Bioresour. Technol. 282, 294–300. https://doi.org/10.1016/J.BIORTECH.2019.03.025.
Shen, Y., Zhang, N., Fu, Y., 2019. Synthesis of high-performance hierarchically porous carbons from rice husk for sorption of phenol in the gas phase. J. Environ. Manage. 241, 53–58. https://doi.org/10.1016/j.jenvman.2019.04.012.
Sheth, Y., Dharaskar, S., Khalid, M., Sonawane, S., 2021. An environment friendly approach for heavy metal removal from industrial wastewater using chitosan based biosorbent: a review. Sustain. Energy Technol. Assessments. 43, 100951 https://doi.org/10.1016/j.seta.2020.100951.
Shi, J., Yan, N., Cui, H., Liu, Y., Weng, Y., 2017. Sulfur doped microporous carbons for CO2 adsorption. J. Environ. Chem. Eng. 5, 4605–4611. https://doi.org/10.1016/J.JECE.2017.09.002.
Sigot, L., Ducom, G., Benadda, B., Labouré, C., 2014. Adsorption of octamethylcyclotetrasiloxane on silica gel for biogas purification. Fuel 135, 205–209. https://doi.org/10.1016/j.fuel.2014.06.058.
Sigot, L., Ducom, G., Benadda, B., Labouré, C., 2016. Comparison of adsorbents for H 2S and D4 removal for biogas conversion in a solid oxide fuel cell. Environ. Technol. (United Kingdom). 37, 86–95. https://doi.org/10.1080/09593330.2015.1063707.
Słupek, E., Makoś, P., 2020. Absorptive desulfurization of model biogas stream using choline chloride-based deep eutectic solvents. Sustainability 12, 1619–1635. https://doi.org/10.3390/su12041619.

Smet, E., Lens, P., Van Langenhove, H., 1998. Treatment of waste gases contaminated with odorous sulfur compounds. Crit. Rev. Environ. Sci. Technol. 28, 89–117. https://doi.org/10.1080/10643389891254179.
Stöcker, M., 2023. Perspectives for thermochemical conversions of lignocellulosic biomass. Small 2302495, 1–9. https://doi.org/10.1002/smll.202302495.
Su, C., Guo, Y., Chen, H., Zou, J., Zeng, Z., Li, L., 2020. VOCs adsorption of resin-based activated carbon and bamboo char: porous characterization and nitrogen-doped effect. Colloids Surfaces A Physicochem. Eng. Asp. 601, 124983 https://doi.org/10.1016/j.colsurfa.2020.124983.
Su, W., Yao, L., Ran, M., Sun, Y., Liu, J., Wang, X., 2018. Adsorption properties of N2, CH4, and CO2 on sulfur-doped microporous carbons. J. Chem. Eng. Data 63, 2914–2920. https://doi.org/10.1021/acs.jced.8b00227.
Sun, Y., Jia, J., Huo, L., Zhao, L., Yao, Z., Liu, Z., 2023. Heteroatom-doped biochar for CO2 adsorption: a review of heteroatoms, doping methods, and functions. Biomass Convers. Biorefinery. https://doi.org/10.1007/s13399-022-03640-5.
Surra, E., Costa Nogueira, M., Bernardo, M., Lapa, N., Esteves, I., Fonseca, I., 2019. New adsorbents from maize cob wastes and anaerobic digestate for H2S removal from biogas. Waste Manag. 94, 136–145. https://doi.org/10.1016/j.wasman.2019.05.048.
Švábová, M., Bičáková, O., Vorokhta, M., 2023. Biochar as an effective material for acetone sorption and the effect of surface area on the mechanism of sorption. J. Environ. Manage. 348 https://doi.org/10.1016/j.jenvman.2023.119205.
Tan, Z., Yuan, S., Hong, M., Zhang, L., Huang, Q., 2020. Mechanism of negative surface charge formation on biochar and its effect on the fixation of soil Cd. J. Hazard. Mater. 384, 121370 https://doi.org/10.1016/J.JHAZMAT.2019.121370.
Tariq, W., Arslan, C., Tayyab, N., Rashid, H., Nasir, A., 2023. Application of agro-based adsorbent for removal of heavy metals. Emerg. Tech. Treat. Toxic Met. from Wastewater. 157–182. https://doi.org/10.1016/B978-0-12-822880-7.00008-X.
Tomul, F., Arslan, Y., Kabak, B., Trak, D., Tran, H.N., 2021. Adsorption process of naproxen onto peanut shell-derived biosorbent: important role of n–π interaction and van der Waals force. J. Chem. Technol. Biotechnol. 96, 869–880. https://doi.org/10.1002/jctb.6613.
Tran, T.M., Hoang, A.Q., Le, S.T., Minh, T.B., Kannan, K., 2019. A review of contamination status, emission sources, and human exposure to volatile methyl siloxanes (VMSs) in indoor environments. Sci. Total Environ. 691, 584–594. https://doi.org/10.1016/J.SCITOTENV.2019.07.168.
Tripathi, M., Sahu, J.N., Ganesan, P., 2016. Effect of process parameters on production of biochar from biomass waste through pyrolysis: a review. Renew. Sustain. Energy Rev. 55, 467–481. https://doi.org/10.1016/j.rser.2015.10.122.
Tyagi, U., Anand, N., 2023. Prospective of waste lignocellulosic biomass as precursors for the production of biochar: application, performance, and mechanism—a review. Bioenergy Res. 16, 1335–1360. https://doi.org/10.1007/s12155-022-10560-9.
U.S. Environmental Protection Agency (EPA), 2024. What are volatile organic compounds (VOCs)? https://www.epa.gov/indoor-air-quality-iaq/what-are-volatile-organic-compounds-vocs.
Varjani, S., Joshi, R., Srivastava, V.K., Ngo, H.H., Guo, W., 2020. Treatment of wastewater from petroleum industry: current practices and perspectives. Environ. Sci. Pollut. Res. 27, 27172–27180. https://doi.org/10.1007/s11356-019-04725-x.
Vikrant, K., Kim, K.H., Peng, W., Ge, S., Sik Ok, Y., 2020. Adsorption performance of standard biochar materials against volatile organic compounds in air: a case study using benzene and methyl ethyl ketone. Chem. Eng. J. 387, 123943 https://doi.org/10.1016/j.cej.2019.123943.
Wang, B., Yang, W., McKittrick, J., Meyers, M.A., 2016. Keratin: structure, mechanical properties, occurrence in biological organisms, and efforts at bioinspiration. Prog. Mater. Sci. 76, 229–318. https://doi.org/10.1016/J.PMATSCI.2015.06.001.
Wang, G., Zhang, Z., Hao, Z., 2019. Recent advances in technologies for the removal of volatile methylsiloxanes: a case in biogas purification process. Crit. Rev. Environ. Sci. Technol. 49, 2257–2313. https://doi.org/10.1080/10643389.2019.1607443.
Wang, H., Shao, Y., Mei, S., Lu, Y., Zhang, M., Sun, J.K., Matyjaszewski, K., Antonietti, M., Yuan, J., 2020a. Polymer-derived heteroatom-doped porous carbon materials. Chem. Rev. 120, 9363–9419. https://doi.org/10.1021/acs.chemrev.0c00080.
M. Wang, Study of Volatile Organic Compounds (VOC) in the cloudy atmosphere: air / droplet partitioning of VOC To cite this version: HAL Id: tel-02864762 PhD Thesis, (2020).
Wang, N., Tan, L., Xie, L., Wang, Y., Ellis, T., 2020b. Investigation of volatile methyl siloxanes in biogas and the ambient environment in a landfill. J. Environ. Sci. 91, 54–61. https://doi.org/10.1016/J.JES.2020.01.005.
Wang, S., Dai, G., Yang, H., Luo, Z., 2017a. Lignocellulosic biomass pyrolysis mechanism: a state-of-the-art review. Prog. Energy Combust. Sci. 62, 33–86. https://doi.org/10.1016/j.pecs.2017.05.004.
Wang, Y., Zuo, S., Yang, J., Yoon, S.H., 2017b. Evolution of phosphorus-containing groups on activated carbons during heat treatment. Langmuir 33, 3112–3122. https://doi.org/10.1021/acs.langmuir.7b00095.
Wang, Y., Chen, W., Zhao, B., Wang, H., Qin, L., Han, J., 2020c. Preparation of high-performance toluene adsorbents by sugarcane bagasse carbonization combined with surface modification. RSC Adv. 10, 23749–23758. https://doi.org/10.1039/d0ra02225j.
Wang, Y., Ma, C., Liu, Y., 2023. Oxidation absorption of nitric oxide from flue gas using biochar-activated peroxydisulfate technology. Fuel 337, 127189. https://doi.org/10.1016/J.FUEL.2022.127189.
Wei, H., Deng, S., Hu, B., Chen, Z., Wang, B., Huang, J., Yu, G., 2012. Granular bamboo-derived activated carbon for high CO2 adsorption: the dominant role of narrow micropores. ChemSusChem 5, 2354–2360. https://doi.org/10.1002/cssc.201200570.
Wohlgemuth, S.A., White, R.J., Willinger, M.G., Titirici, M.M., Antonietti, M., 2012. A one-pot hydrothermal synthesis of sulfur and nitrogen doped carbon aerogels with enhanced electrocatalytic activity in the oxygen reduction reaction. Green Chem. 14, 1515–1523. https://doi.org/10.1039/c2gc35309a.
Wu, J., Zhu, X., Yang, F., Wang, R., Ge, T., 2022. Shaping techniques of adsorbents and their applications in gas separation: a review. J. Mater. Chem. A 10, 22853–22895. https://doi.org/10.1039/d2ta04352a.
Xiang, W., Zhang, X., Chen, K., Fang, J., He, F., Hu, X., Tsang, D.C.W., Ok, Y.S., Gao, B., 2020. Enhanced adsorption performance and governing mechanisms of ball-milled biochar for the removal of volatile organic compounds (VOCs). Chem. Eng. J. 385, 123842 https://doi.org/10.1016/J.CEJ.2019.123842.
Xiao, L.P., Shi, Z.J., Xu, F., Sun, R.C., 2012. Hydrothermal carbonization of lignocellulosic biomass. Bioresour. Technol. 118, 619–623. https://doi.org/10.1016/j.biortech.2012.05.060.
Xie, L., Yang, D., Lu, Q., Zhang, H., Zeng, H., 2020. Role of molecular architecture in the modulation of hydrophobic interactions. Curr. Opin. Colloid Interface Sci. 47, 58–69. https://doi.org/10.1016/J.COCIS.2019.12.001.
Xue, S., Ding, W., Li, L., Ma, J., Chai, F., Liu, J., 2022. Emission, dispersion, and potential risk of volatile organic and odorous compounds in the exhaust gas from two sludge thermal drying processes. Waste Manag. 138, 116–124. https://doi.org/10.1016/J.WASMAN.2021.11.040.
Yakout, S.M., 2015. Monitoring the changes of chemical properties of rice straw-derived biochars modified by different oxidizing agents and their adsorptive performance for organics. Biorem. J. 19, 171–182. https://doi.org/10.1080/10889868.2015.1029115.
Yang, F., Li, W., Ou, R., Lu, Y., Dong, X., Tu, W., Zhu, W., Wang, X., Li, L., Yuan, A., Pan, J., 2022. Superb VOCs capture engineering carbon adsorbent derived from shaddock peel owning uncompromising thermal-stability and adsorption property. Chin. J. Chem. Eng. 47, 120–133. https://doi.org/10.1016/j.cjche.2021.02.013.
Yang, H., Dong, Z., Liu, B., Chen, Y., Gong, M., Li, S., Chen, H., 2021. A new insight of lignin pyrolysis mechanism based on functional group evolutions of solid char. Fuel 288, 119719. https://doi.org/10.1016/j.fuel.2020.119719.
Yang, Y., Qu, X., Huang, G., Ren, S., Dong, L., Sun, T., Liu, P., Li, Y., Lei, T., Cai, J., 2023. Insight into lignocellulosic biomass torrefaction kinetics with case study of pinewood sawdust torrefaction. Renew. Energy 215, 118941. https://doi.org/10.1016/J.RENENE.2023.118941.
Yao, X., Zhou, J., Liu, Z., 2022a. Study on adsorption of low-concentration methyl mercaptan by starch-based activated carbon. Chemosphere 302, 134901. https://doi.org/10.1016/j.chemosphere.2022.134901.
Yao, X., Shi, Y., Zhou, J., Yao, Z., Li, C., He, L., Gong, W., 2022b. Effects of water vapor on adsorption performance of activated carbon for methyl Mercaptan, toluene and N-hexane in fermentation industrial waste gas. SSRN Electron. J. 1–25. https://doi.org/10.2139/ssrn.4250702.
Ye, Q., Chen, Y., Li, Y., Jin, R., Geng, Q., Chen, S., 2023. Management of typical VOCs in air with adsorbents: status and challenges. Dalt. Trans. 52, 12169–12184. https://doi.org/10.1039/d3dt01930f.
Yu, X., Liu, S., Lin, G., Zhu, X., Zhang, S., Qu, R., Zheng, C., Gao, X., 2018. Insight into the significant roles of microstructures and functional groups on carbonaceous surfaces for acetone adsorption. RSC Adv. 8, 21541–21550. https://doi.org/10.1039/c8ra03099e.
Zeghioud, H., Fryda, L., Djelal, H., Assadi, A., Kane, A., 2022. A comprehensive review of biochar in removal of organic pollutants from wastewater: characterization, toxicity, activation/functionalization and influencing treatment factors. J. Water Process Eng. 47, 102801 https://doi.org/10.1016/j.jwpe.2022.102801.
Zhang, C., Wang, M., Chen, W.H.H., Zhang, Y., Pétrissans, A., Pétrissans, M., Ho, S.H.H., 2023. Superhydrophobic and superlipophilic biochar produced from microalga torrefaction and modification for upgrading fuel properties. Biochar 5. https://doi.org/10.1007/s42773-023-00217-x.
Zhang, H., Wang, X., Shen, X., Li, X., Wu, B., Li, G., Bai, H., Cao, X., Hao, X., Zhou, Q., Yao, Z., 2022a. Chemical characterization of volatile organic compounds (VOCs) emitted from multiple cooking cuisines and purification efficiency assessments. J. Environ. Sci. https://doi.org/10.1016/J.JES.2022.08.008.
Zhang, N., Shen, Y., 2019. One-step pyrolysis of lignin and polyvinyl chloride for synthesis of porous carbon and its application for toluene sorption. Bioresour. Technol. 284, 325–332. https://doi.org/10.1016/j.biortech.2019.03.149.
Zhang, X., Gao, B., Zheng, Y., Hu, X., Creamer, A.E., Annable, M.D., Li, Y., 2017b. Biochar for volatile organic compound (VOC) removal: sorption performance and governing mechanisms. Bioresour. Technol. 245, 606–614. https://doi.org/10.1016/j.biortech.2017.09.025.
Zhang, X., Gao, B., Fang, J., Zou, W., Dong, L., Cao, C., Zhang, J., Li, Y., Wang, H., 2019. Chemically activated hydrochar as an effective adsorbent for volatile organic compounds (VOCs). Chemosphere 218, 680–686. https://doi.org/10.1016/j.chemosphere.2018.11.144.
Zhang, X., Xiang, W., Wang, B., Fang, J., Zou, W., He, F., Li, Y., Tsang, D.C.W., Ok, Y.S., Gao, B., 2020. Adsorption of acetone and cyclohexane onto CO2 activated hydrochars. Chemosphere 245, 125664. https://doi.org/10.1016/j.chemosphere.2019.125664.
Zhang, X., Miao, X., Xiang, W., Zhang, J., Cao, C., Wang, H., Hu, X., Gao, B., 2021. Ball milling biochar with ammonia hydroxide or hydrogen peroxide enhances its adsorption of phenyl volatile organic compounds (VOCs). J. Hazard. Mater. 403, 123540 https://doi.org/10.1016/j.jhazmat.2020.123540.
Zhang, X., Gang, D.D., Zhang, J., Lei, X., Lian, Q., Holmes, W.E., Zappi, M.E., Yao, H., 2022b. Insight into the activation mechanisms of biochar by boric acid and its application for the removal of sulfamethoxazole. J. Hazard. Mater. 424, 127333 https://doi.org/10.1016/J.JHAZMAT.2021.127333.

Zhang, X., Cao, L., Xiang, W., Xu, Y., Gao, B., 2022c. Preparation and evaluation of fine-tuned micropore biochar by lignin impregnation for CO2 and VOCs adsorption. Sep. Purif. Technol. 295, 121295 https://doi.org/10.1016/j.seppur.2022.121295.
Zhang, Y., Chen, P., Liu, S., Peng, P., Min, M., Cheng, Y., Anderson, E., Zhou, N., Fan, L., Liu, C., Chen, G., Liu, Y., Lei, H., Li, B., Ruan, R., 2017a. Effects of feedstock characteristics on microwave-assisted pyrolysis – a review. Bioresour. Technol. 230, 143–151. https://doi.org/10.1016/J.BIORTECH.2017.01.046.
Zhao, X., Zeng, X., Qin, Y., Li, X., Zhu, T., Tang, X., 2018. An experimental and theoretical study of the adsorption removal of toluene and chlorobenzene on coconut shell derived carbon. Chemosphere 206, 285–292. https://doi.org/10.1016/J.CHEMOSPHERE.2018.04.126.
Zhao, Z., Wang, B., Theng, B.K.G., Lee, X., Zhang, X., Chen, M., Xu, P., 2022. Removal performance, mechanisms, and influencing factors of biochar for air pollutants: a critical review. Biochar 4, 1–24. https://doi.org/10.1007/s42773-022-00156-z.
Zhou, S., Wang, M., Wang, J., Xin, H., Liu, S., Wang, Z., Wei, S., Lu, X., 2020. Carbon phosphides: promising electric field controllable nanoporous materials for CO2capture and separation. J. Mater. Chem. A 8, 9970–9980. https://doi.org/10.1039/d0ta03262j.
Zhou, X., Zhou, X., Wang, C., Zhou, H., 2023. Environmental and human health impacts of volatile organic compounds: a perspective review. Chemosphere 313, 137489. https://doi.org/10.1016/j.chemosphere.2022.137489.
Zhu, J., Li, Y., Xu, L., Liu, Z., 2018. Removal of toluene from waste gas by adsorption-desorption process using corncob-based activated carbons as adsorbents. Ecotoxicol. Environ. Saf. 165, 115–125. https://doi.org/10.1016/j.ecoenv.2018.08.105.
Zhu, L., Shen, D., Luo, K.H., 2020. A critical review on VOCs adsorption by different porous materials: species, mechanisms and modification methods. J. Hazard. Mater. 389, 122102 https://doi.org/10.1016/J.JHAZMAT.2020.122102.
Zhuang, Z., Wang, L., Tang, J., 2021. Efficient removal of volatile organic compound by ball-milled biochars from different preparing conditions. J. Hazard. Mater. 406, 124676 https://doi.org/10.1016/j.jhazmat.2020.124676.
Zulkefli, N.N., Shahbudin, M., Id, M., Nor, W., Wan, R., Jahim, J., Rejab, S.A., Lye, C.C., 2019. Removal of hydrogen sulfide from a biogas mimic by using impregnated activated carbon adsorbent. PloS One 14 (2), e0211713.